A GENETIC AND MINERALOGICAL STUDY OF TWO SOILS FROM THE DAVIS MOUNTAIN REGION, TEXAS

by

Larry Felder Ratliff, B.S.

A THESIS

IN

AGRONOMY

Submitted to the Graduate Committee
of Texas Technological College
in Partial Fulfillment of
the Requirements for
the Degree of

MASTER OF SCIENCE IN AGRICULTURE

Approved

Accepted

June, 1968

ACKNOWLEDGEMENTS

The author would like to express his deepest gratitude to Dr. B. L. Allen for his counsel, translation of Italian literature, and encouragement during preparation of this thesis. The help of Dr. W. T. Parry, Geosciences Department, and Dr. R. E. Meyer, Agronomy Department, graduate committee members, is also deeply appreciated.

Sincere thanks are due to Mr. Horace Dean and Mr. August Turner, Soil Conservation Service soil scientists, for their help in selecting and sampling the soils.

TABLE OF CONTENTS

LIST OF TABLES

LIST OF ILLUSTRATIONS

LIST OF ILLUSTRATIONS

continued

CHAPTER I

INTRODUCTION

The primary purpose of this study was to acquire information concerning the genesis of two soils developed from volcanic materials. Secondary objectives were to establish modal profiles for use in classification of the soils.

In order to accomplish these objectives, special emphasis was placed on the mineralogical changes brought about by weathering processes. These mineralogical changes involve the physical breakdown and chemical decomposition of the parent material, alteration of primary minerals, and in some cases, the synthesis of new minerals. The weathering processes; solution, hydration, hydrolysis, oxidation, reduction, carbonation, cation-anion exchange reactions, etc., are a part of soil formation and are responsible for the transformation of a parent material into a soil. The degree of change in a parent material brought about by weathering processes is influenced by the soil forming factors; nature of the parent material, climate, topography or relief, organisms, and time. Consideration of the soil and parent material mineralogy in conjunction with the soil forming factors should reflect the genesis of the soil in question.

In the two soils selected for study, only the soil forming factors; time, organisms, and perhaps climate, were considered to be constant. The soils occupied distinctively different topographic positions and are developing from different types of parent material. One soil is developing from trachytic bedrock on a relatively flat mesa top whil

the other is forming from trachytic and rhyolitic valley-fill debris in a broad intermontane basin. Slight climatic differences between the two soils result from the difference in relief.

The conclusions drawn in this investigation were based on the physical and chemical properties of the soils determined in the laboratory and the morphological studies made in the field.

CHAPTER II

REVIEW OF LITERATURE

Geography of the Davis Mountains

The triangular section of Texas west of the Pecos River, bounded on the south and west by the Republic of Mexico and on the north by New Mexico is commonly referred to as the Trans-Pecos region. This region is unique since it contains all of Texas' true mountains. The Trans-Pecos mountain ranges cross the western extension of Texas in a general north-south direction and continue along the eastern edge of the high central plateau of Mexico.

Within these mountain ranges, the Davis Mountains occupy an irregularly shaped area of approximately 1400 square miles in Jeff Davis, Brewster, and Presidio counties in the west central Trans-Pecos. They lie at the north end of the Eastern Border Ranges division of the Mexican Highlands (33). Along the east side of the southern Davis Mountains is the Marathon dome which is formed by the Del Norte and Santiago Mountains. The Davis Mountains are bounded on the north by the Apache Mountains and on the west by a broad, relatively undissected, plain which grades into the Van Horn and Tierra Vieja Mountains. The Barrilla Mountains lie to the northeast and are actually a northeastward outlier of the Davis Mountains although a pronounced syncline separates the two.

The Davis Mountains intercept moisture bearing winds and cause more precipitation than elsewhere in the Trans-Pecos region. Jeff Davis County has the highest average elevation among Texas counties, the

altitude ranging from 3800-5200 feet. The average annual rainfall is 18.72 inches and the mean average temperature is 56.5 degrees Fahrenheit. The rainfall is seasonal, approximately 75% falling in May through September (40).

Geology of the Davis Mountains

The Davis Mountains are a highly dissected erosional remnant of a vast volcanic field that may have originally covered several thousand square miles in Trans-Pecos, Texas and northern Mexico (33). Thick volcanic successions were believed to have accumulated in the northeastern part of an extensive structural depression bounded on the north by the Apache-Delaware uplift and on the east by the Marathon dome. Differential erosion has since carved the area into rugged mountain terrain. Several investigators (14, 25, 43) state that the present mountains owe their origin to the effects of erosion on the lava flows that have covered the area. They are remnants of a broad plateau which was gently folded and severely dissected. Hawley (J. W. Hawley, unpublished field report), in describing geologic events pertinent to the formation of the Davis Mountains, states that early to middle Cenozoic volcanism and structural deformation resulted in the basic outlines of the Basin and Range province of the Mexican highlands. Regional uplift, block-faulting, erosion of upland masses, and filling of closed intermontane basins prevailed through late Tertiary time. Significant tectonic distrubances probably ceased by the beginning of the Quaternary period and erosion of uplands with subsequent filling of basins has since prevailed. Huang and Craft (23) propose that the

following sequence of events was possible in the Davis Mountain area.

> 1) Laramide uplift and orogeny between late Cretaceous and Paleocene; 2) outpourings of trachyte and tuff deposition in the Eocene; 3) extrusions of basic lavas during early Oligocene; 4) intermittent volcanism and eruption of lavas and rhyolitic tuff that were interspersed with sedimentation during early or middle Miocene; 5) regional uplift and development of the Duff Springs formation during late Pliocene and early Pleistocene; 6) outpourings of plateau rhyolites, tuffs, and younger basalts followed by syenite intrusions in early Pleistocene.

Huang and Craft's work is the most precise attempt at dating recent geologic events which occurred in the Davis Mountain region. Other investigators (17, 25) have placed the dates of the volcanism as Eocene, Oligocene, and possibly Miocene. The few fossils found, in isolated sedimentary lenses within the lavas, were not diagnostic and the precise geologic time is indefinite (17, 25). However, all investigators have generally agreed that the volcanic activity was early Tertiary.

Numerous investigations (4, 10, 15, 25, 33, 36) within and around the Davis Mountain area reveal a variety of rock types that are exposed. Precambrian metaquartzites, metaarkoses, and schists are exposed in the Van Horn Mountains to the north. In the northern Davis Mountains, sedimentary rocks which are predominantly Cretaceous limestones are evident. The bulk of the exposed rock in the area, however, consists of fine grained volcanic rocks of Tertiary age.

Hawley (J. W. Hawley, unpublished field report) in a review of the volcanic rocks present in the Jeff Davis County area states that both lavas and pyroclastic rocks are prevalent. The lavas range from rhyolite and trachyte to basalt. The rhyolites contain abundant quartz and potas

feldspar whereas the trachytes are low in quartz and high in sodic and potash feldspar. The basalts are high in calcic-sodic feldspar and ferromagnesian minerals. Tuffs, often indurated, are the most common pyroclastic rocks and are often interbedded in the lavas. The pyroclastic rocks are mainly rhyolitic. Vogel (43) states that the igneous rocks in the southwestern Davis Mountains are mainly rhyolitic lava flows, tuffs, and volcanic ash. The lavas are massive, jointed, and are all more or less porphyritic. The dominant phenocrysts were identified as feldspars. Tuff breccias, agglomerates and conglomerates are interbedded with the lavas. The tuffs described as containing large amounts of fine grained quartz, were believed to have undergone considerable weathering and hydrothermal metamorphism in localized areas.

Eifler (16) states that alternating layers of early Tertiary age tuffs overlie marine Upper Cretaceous strata in structurally low areas. Uplifts on the north, east, and west have exposed Lower Cretaceous and Permian rocks. Southward, the Davis Mountains merge with well dissected, alluvium covered tuffs. The Davis Mountains closely resemble the Barrilla Mountains which lie to the northeast. The Tertiary system of the Barrilla Mountains is composed of the Huelster formation, Star Mountain rhyolite, and the Seven Springs formation. The Huelster formation is principally composed of tuff; the Star Mountain rhyolite is principally a thick lava layer; and the Seven Springs formation consists of eight alternating layers of tuff and lava. These volcanic rocks range from 1500 to 1700 feet in thickness. Jones (25) in an earlier investigation of the Barrilla Mountains also identified ten alternating layers of tuff and lavas whose combined thickness was 1500 feet. This igneous section

thickens westward in the Davis Mountains. This investigator states that the lava flows of the Barrilla and eastern Davis Mountains undergo a lithologic change from rhyolites below to trachytes above. The separate lava flows appear to maintain their own common characteristics and cover extensive areas. The lava flows thicken toward the west and southwest, thus indicating that the source of the flows must have been in that direction. Jones states that the lava source is believed to have been in the Davis Mountain area west of Fort Davis.

As previously indicated, the Davis Mountains are erosional remnants of a vast volcanic field. Several investigators (1, 14, 15, 16) have attempted to characterize the alluvial sediments which have been deposited in the broad intermontane and smaller upland valleys of the Davis Mountain area. The geologic date of these deposits is generally considered to be Quaternary although some reference is occasionally made to late Tertiary.

The most extensive investigation of the alluvial sediments in the Davis Mountain area is that of Albritton and Bryan (1). The open plain-like valleys in the southern Davis Mountains and outlying country to the west, south, and east are essentially eroded surfaces that are veneered by Quaternary alluvium. The average thickness of this alluvium is 20 feet and is divisible into three distinct bodies by the presence of disconformities. Albritton and Bryan assigned the names of Neville, Calamity, and Kokernot to the formations; the Neville being the oldest and the Kokernot the youngest. These investigators found that generally, the Neville formation can be distinguished from the younger alluvium by its more compact nature, greater content of clay and fine silt, prevailing

reddish brown color, and by its higher content of secondary calcium carbonate in the form of nodules and cement. The intermediate layer, the Calamity, contains more gravel and less caliche than the Neville. The Calamity tends to be dark gray in color because of the presence of humic materials. The Kokernot contains no visible caliche and consists of uncemented and highly irregular deposits of sand and gravel.

Albritton and Bryan described the alluvial sediments which had been deposited in a triangular area bounded by Valentine, Fort Davis, and Ryan, Texas. (Ryan is a railroad depot which lies midway between Valentine and Marfa on the Southern Pacific railroad.) One site described by Albritton and Bryan is of particular interest since it lies approximately 10 miles to the northwest of the area where the Musquiz soil was sampled. The site described by Albritton and Bryan is presented below.

Quaternary	Thickness in Feet
Kokernot formation	
8. Unconsolidated gray silt and fine sand	0.1
Disconformity	
Calamity formation	
7. Dark humic gritty silt	2.0
6. Reddish to buff gritty silt	2.0
5. Pebbly humic silt and clay with columnar fracture	2.5
4. Pebble and cobble gravel	0.5
3. Carbonaceous grit containing hearths and abundant charcoal	1.0
2. Reddish-brown to gray silt interbedded with sand and gravel; contains bits of charcoal	5
Disconformity	

	Thickness in Feet
Neville formation	
1. Silty clay with interbedded pebble and cobble gravel; color, blush	0-10
Total exposed thickness	16
Unconformity	
Tertiary bedrock	

The Neville rests unconformably on bedrock and covers wide areas in the extensive plain-like valleys of the area. The Calamity fills wide, but well defined, channels that were cut into the Neville. The Kokernot is generally confined to constricted channel cuts in the Calamity formation. Albritton and Bryan (1) and DeFord (15) state that the three formations record three separate aggradations in the valleys and that the disconformities between formations record erosional periods. Albritton and Bryan state that a third cycle of channeling began after the Kokernot deposition and continues until the present. Recent arroyos have followed the lines of least resistance so that almost all of the Kokernot, except for thin flood phases, has been destroyed.

Rhyolite and Trachyte-Derived Soils

In a mineralogical study of soil formation it is advantageous to consider the nature of the parent rock since the mineralogy of the rock is often directly reflected in the soil properties. Field studies and preliminary laboratory investigations indicate that the two soils under study were developed from rhyolitic or trachytic material. A review of existing literature revealed that few reports of soils forming from rhyolites

or trachytes exist. Some of the existing reports were not considered pertinent to this study because of obvious differences in the degree of weathering of the soils.

Swindale and Jackson (39) in 1960, published a resume of a study of four rhyolite derived soils from New Zealand. They gave detailed descriptions of the mineralogy of the sand, silt, and clay fractions. The four soils described were in different weathering stages, ranging from low to moderately weathered, to strongly weathered and strongly podzolized. Two of the soils, the Koikoi and Maungarei, were believed to be weakly weathered and strongly weathered, respectively, but little affected by the processes of podzolization. The rhyolite from which these two soils were developed had porphyritic textures, the phenocrysts ranging in size from 1.0 millimeter (mm.) to 0.1 mm. The groundmass varied from wholly crystalline to glassy.

The sand fraction of the Koikoi soil contained primary quartz, feldspar, and volcanic glass. The feldspars were predominantly sanidine and oligoclase. The silt fractions also contained large quantities of feldspar and quartz with minute amounts of mica, chlorite, vermiculite, and montmorillonite. Sanidine was the dominant feldspar species. The mineralogy of the coarse clay (2 to 0.2 microns) was very similar to that of the silts except that there was a decrease in feldspars and significant quantities (19 to 24%) of kaolin were present. The fine clays, less than 0.2 microns, ($<0.2\mu$) contained smaller amounts of primary minerals and kaolinite but increased quantities of mica, chlorite, and expanding layer silicates. Most of the 2:1 and 2:2 layer silicates were discrete but X-ray analysis also revealed some interstratification

of mica, vermiculite, and chlorite. It was proposed by Swindale and Jackson that the Koikoi parent material contained sufficient potassium (K) and magnesium (Mg) to allow mica, chlorite, and expanding 2:1 layer silicates to form but insufficient K and Mg to preclude the formation of kaolin.

The Maungarei soil was apparently formed under a moderate to high degree of weathering and most of the primary minerals, other than quartz, had been decomposed. The sand fractions contained quartz, oligoclase, and small quantities of sanidine. Quartz was the dominant mineral of the silt fractions but feldspars, cristobalite, and layer silicates with primary basal spacings of 14, 10, and 7 angstroms (A) were present. The coarse clays were predominantly kaolin. The fine clays were mainly composed of halloysitic kaolin but had significant quantities of mica, chlorite, and expanding layer silicates. The preponderance of kaolin minerals in the clay fractions was attributed to the weathering stage of the soil.

Although disseminated throughout the profiles, the percentage extractable Fe_2O_3 was notably low for both soils. The quartz was primarily concentrated in the fine sand, silt, and coarse clay fractions. This was attributed to the microcrystalline texture of the rhyolite.

The discussion of Swindale and Jackson concerning the rhyolite derived soils which had been formed by strong weathering and moderate to strong podzolization processes is not considered directly pertinent to this study. However, a general examination of the mineralogy of the soils indicated that continued weathering of an already strongly weathered soil results in the breakdown of kaolin minerals, formation

of gibbsite, and concentration of quartz. Iron, liberated from primary minerals, was precipitated as hydrous oxides and was also concentrated as other materials were removed by leaching.

The study made by Swindale and Jackson show that the degree of weathering which a rhyolite derived soil has undergone determines, to some extent, the mineralogy. Apparently, such soils which are weakly to moderately weathered contain considerable quantities of primary minerals and mixed, secondary layer silicates such as mica, chlorite, vermiculite, montmorillonite, kaolin, and interstratified clay types. The proportion of each clay type varies with the concentration of such ions as K and Mg and also the silica/alumina ratios. Continued weathering of the soils, loss of K, Mg, etc., provides a favorable environment for kaolin formation and this clay mineral becomes dominant. With time and continued weathering, the kaolin may be destroyed and concentrations of resistant primary and secondary minerals occur.

Van der Marel (31) found that the rhyolitic tuff which fell at Sumatra's East Coast from the Toba eruption contained quartz, sanidine, volcanic glass, and weathered biotite in the light mineral, specific gravity (s.g.) <2.89, fraction. Minerals identified in the heavy mineral fraction, greater than (>) 2.89 s.g., were amphibole, hypersthene, allanite, zircon, and unweathered biotite. This investigator stated that it was possible to use the heavy mineral fraction in determining the stage of weathering of soils derived from rhyolitic rocks. An extensive study of soils in weathering stages ranging from unweathered tuff to a very strongly weathered soil revealed that the percentages

of allanite and zircon increased with weathering; whereas the percentages of hypersthene and amphiboles decreased as weathering increased. The percentage of ore and opaque minerals increased until the soils were moderately weathered but then decreased as the weathering processes continued.

Carloni and Lotti (13), in 1960, reported the results of study of eleven soil samples taken from four different soils developing over trachyte in the Pisa Livorno and Grosseto regions, Italy. The trachyte was of two different types, one they called "toscaniti" and the other was designated "selagita". The actual difference between the two types of trachyte was not specified, but they were both reported to contain skeletal fragments of sanidine and biotite. Mechanical analysis revealed that the clay fraction (<2 microns) composed less than 10% of the whole soil for all samples. X-ray, differential thermal, and chemical analyses revealed a somewhat mixed clay mineralogy. Illite was identified in all samples and kaolinite was found in all but three samples. The samples which did not contain kaolinite were dominated by a clay mineral believed to be an irregular interstratified montmorillonite-vermiculite. Accessory minerals in the clay fractions were quartz, goethite, diaspore, and boehmite. As would be expected, the soils dominated by the interstratified clay type had significantly higher cation exchange capacities than those containing only illite or kaolinite. Carloni and Lotti gave no indication of the maturity of the soils examined, but low clay contents indicated that the soils were relatively immature.

In a similar study, Buondonno and Violante (12) found that the dominant clay type in soils developed from sanidine tuff, believed to

be trachytic, in the Irno Valley of Italy was halloysite and meta-halloysite. Other clay minerals frequently noted were illite and an interstratified clay type. The components of the interstratified clay type were not identified. The tuffs were composed of sanidine, augite, biotite, magnetite, pumice, and lapilli. These investigators indicated that the soils examined were, in general, porous and were believed to contain significant quantities of amorphous materials.

Several investigators (3, 6, 7) have reported the presence of amorphous materials, principally allophane, in soils derived from andesitic and rhyolitic volcanic ash. Birrel and Fieldes (3) found that older New Zealand soils derived from volcanic ash contained halloysite or kaolin minerals which had almost certainly been formed from allophane by crystallization.

CHAPTER III

FIELD STUDIES

Representative profiles of two soil series that have been tentatively named Kokernot and Musquiz were described and sampled. These soils occupy two distinct topographic localities in the Davis Mountain region of Texas. The Kokernot soil is found on nearly level mesa tops of volcanic origin whereas the Musquiz soil characteristically develops in broad intermontane valleys.

The profiles were sampled and described on September 8-9, 1966, with the help of Dr. B. L. Allen, Professor of Soils at Texas Technological College, Mr. Horace Dean, Field Specialist-Soils for the Soil Conservation Service, and Mr. August Turner, Soil Scientist for the Soil Conservation Service.

Samples, including peds and pebbles, were taken of each horizon described. Three auger samples were taken at intervals below the Musquiz IIClca horizon. These samples were taken to provide additional information on the parent material. The samples were differentiated by color and texture changes and thus designated IIC2, IIIC3ca, and IIIC4 horizons. Only the depths at which the horizons were sampled are noted in the profile description.

The descriptions were made using the nomenclature of the 7th Approximation (37). Pictures were made of each site and profile and are shown in Figures 1, 2, 3, and 4.

Field Characteristics

There was no evidence at either site of significant profile

Figure 1.--Landscape at Kokernot site.

Figure 2.--Profile of the Kokernot soil.

disturbance. A one inch layer of recent aeolian material had been deposited at the Musquiz site. This layer was described but not sampled.

Kokernot Soil Description

Location: Texas highway 118 is followed 9.8 miles southeast from the courthouse in Fort Davis. Turn northeast at C. C. Pollard ranch gate and travel 2.5 miles to ranch house. The site is located 3.8 miles east, southeast of the house on Grierson Mesa.

Vegetation: Black grama (Bouteloua eriopoda), blue grama (Bouteloua gracilis), sprucetop grama (Bouteloua chondrosioides), cane bluestem (Andropogon barbinodis), Plains lovegrass (Eragrostis intermedia), prickly pear (Opuntia sp.), Agarita (Berberis trifoliolata), and a few scattered juniper (Juniperus sp.).

Parent Material: Residual trachytic volcanic rock.

Topography: Nearly level mesa top.

Soil Profile:

	(Inches)	
A1	0-3	Brown (7.5YR 4/4) sandy loam, dark brown (7.5YR 3/2) moist; moderate fine granular and subangular blocky structure; slightly hard, friable; plentiful roots; 5% (field estimate) by volume of pebbles less than 0.5 inch in diameter; smooth clear boundary.
B1	3-8	Reddish brown (5YR 5/4) loam, dark reddish brown (5YR 3/4) moist; moderate fine subangular blocky structure; slightly hard, friable; plentiful roots; 5% (field estimate) by volume of coarse fragments mostly less than 0.5 inch diameter; smooth clear boundary.
B21t	8-14	Reddish brown (5YR 5/4) clay loam, dark reddish brown (5YR 3/4) moist; moderate fine subangular blocky structure; mostly pebble controlled; hard, firm; 35% (field estimate) by volume of coarse fragments of 0.25 to 2 inch diameter; plentiful roots; wavy to irregular clear boundary.

R/B22t	14-20	Reddish brown (5YR 5/4) clay loam, dark reddish brown (5YR 4/4) moist; pebble controlled moderate, medium blocky structure; hard, firm; 50% (field estimate) by volume of coarse fragments mostly less than 3 inches diameter; few roots; irregular abrupt boundary.
R	20-26+	Bedrock (trachyte porphyry) with clay seams in the crevices. Weathered in the upper 2 to 3 inches.

Remarks: There were a few very coarse rock fragments scattered throughout the profile.

Musquiz Soil Description

Location: Texas highway 17 is followed 2.2 miles southwest from the courthouse in Fort Davis to its intersection with highway 166. Follow Texas highway 166 west for 8.4 miles and turn left on ranch road. Proceed south for 2.8 miles to fence gate. Site is located 250 yards east and 100 yards north from gate.

Vegetation: Blue grama (Bouteloua gracilis), sand muhly (Muhlenbergia arencia), annual threeawn (Aristida sp.), cane bluestem (Andropogon barbinodis), vine mesquite (Panicum obtusum), and buffalo (Buchloe dactyloides). There are a few widely scattered cholla (Opuntia sp.), acacia (Acacia sp.), and mesquite (Prosopis sp.).

Parent Material: Loamy alluvium derived from volcanic materials.

Topography: About 1% south-facing slope in a broad intermontane valley.

Soil Profile:

(Inches)		
A11	0-1	Brown (7.5YR 5/4) loam, dark brown (7.5YR 3/4) moist; weak fine platy structure; soft, friable; plentiful roots; few fine pebbles; smooth abrupt boundary.

A12	1-6	Reddish brown (5YR 4/3) sandy clay loam, dark reddish brown (5YR 3/3) moist; moderate fine subangular blocky and granular structure; slightly hard, friable; plentiful roots; few fine pebbles; smooth clear boundary.
B21t	6-12	Reddish brown (5YR 4/3) clay, dark reddish brown (5YR 3/3) moist; moderate fine subangular blocky structure; hard, firm; few thin patchy clay films; common roots; few pebbles; smooth clear boundary.
B22t	12-22	Dark red (2.5YR 3/6) clay, dark reddish brown (2.5YR 3/4) moist; compound moderate medium subangular and moderate fine blocky structure; hard, firm; a few continuous clay films; common roots and pebbles; smooth gradual boundary.
B23t	22-30	Dark red (2.5YR 3/6) clay, dark red (2.5YR 3/6) moist; compound moderately weak medium subangular and moderate fine blocky structure; hard, firm; few thin continuous clay films; common roots; many pebbles; wavy abrupt boundary.
IIC1ca	30-46	Light reddish brown (5YR 6/4) silty clay loam, reddish brown (5YR 5/4) moist; structureless; hard, friable; 20% (field estimate) by volume of whitish soft and weakly cemented calcium carbonate concretions; 15% (field estimate) by volume of pebbles; few roots; gradual boundary.
IIC2	46-50	
IIIC3ca	50-61	
IIIC4	61-65	

Remarks: All horizons except the A11 and A12 contain an estimated 5 to 10%, by volume, of angular fragments of porphyritic trachyte and rhyolite.

Figure 3.--Landscape at Musquiz site.

Figure 4.--Profile of the Musquiz soil.

CHAPTER IV

METHODS OF STUDY

Determination of Percentage Gravel

The percentage gravel (>2.0 mm. size) of each soil horizon was determined by utilizing wet and dry sieving procedures. The raw soil sample was first passed through a 10 mesh sieve to separate the >2.0 mm. particles from the <2.0 mm. particles. Many soil particles adhering to the gravel fragments were noted and some horizons contained calcium carbonate concretions. The gravel fragments were placed in plastic containers and shaken in distilled water on a reciprocating shaker. The gravel fragments were then wet sieved, the sieved fraction dried and added to the <2.0 fraction. Oven dry weights of both fractions were obtained and the percentage gravel based on total sample weight was calculated.

Particle Size Distribution

Particle size distribution analyses were made using a modified version of the pipette method outlined by Kilmer and Alexander (28). Since modifications of the procedure were employed, the method will be outlined and discussed.

A 10 gram (gm.) sample of soil, <2.0 mm. size, from each horizon was weighed to 10^{-4} gm. The samples were placed in 1000 milliliter (ml.) beakers, treated with 100 ml. of 10% hydrogen peroxide (H_2O_2), covered with a watch glass, and allowed to stand overnight. The samples were

then heated to accelerate the reaction and to reduce the volume of the H_2O_2 suspension to less than two thirds of its original amount. The H_2O_2 treatment was repeated using 100 ml. increments of 15% and 30% H_2O_2 successively. Visual inspection of the sample indicated that almost all of the organic matter was removed. After treatment with the last increment of H_2O_2, the samples were evaporated nearly to dryness in order to destroy the remaining H_2O_2.

Preliminary investigation indicated the presence of calcium carbonate ($CaCO_3$). The carbonates were removed by treating the samples with increments of 10% hydrochloric acid (HCl). The HCl treatment also served to dissolve some of the reaction products of the H_2O_2 oxidation.

The samples were washed into Buchner funnels containing No. 50 Whatman filter paper. Vacuum was applied and the samples washed with distilled water until the filtrates were free of chlorides as determined by the silver nitrate ($AgNO_3$) test. The samples were then washed into 1000 ml. erlenmeyer flasks and brought to a volume of 500 ml. with distilled water. Exactly 10 ml. increments of 5% sodium hexametaphosphate solution (Calgon) were added and the samples shaken on a reciprocating shaker for 10 hours to induce dispersion.

After dispersion, the samples were washed through a 300 mesh sieve into 1000 ml. hydrometer jars. The sand fractions were retained on the sieve, dried, and weighed. The sand was then fractionated into 2.0 to 1.0 mm. (very coarse sand), 1.0 to 0.5 mm. (coarse sand), 0.5 to 0.25 mm. (medium sand), 0.25 to 0.1 mm. (fine sand), and 0.1 to 0.05 mm. (very fine sand) fractions by shaking on a nest of sieves for 5 minutes. The

fractions were weighed and the percentage of each fraction based on the total sand fraction weight, was determined.

The silts and clays were passed through a 300 mesh sieve into hydrometer jars. The jars were placed in a water bath and brought to a constant temperature of 30 degrees Centigrade (30 C). The volume in the hydrometer jars was brought to 1000 ml. and the samples thoroughly stirred with a hand stirrer made of a perforated metal plate attached to a metal rod. The samples were allowed to stand for the time calculated by Stokes law of sedimentation for a 2.0 micron particle to fall 10 centimeters (cm.). The pipettings and calculations were performed as outlined by Kilmer and Alexander.

In previous particle size analyses in the soils laboratory at Texas Technological College, considerable difficulty was experienced in getting samples to disperse if the samples were dried after treatment with H_2O_2 and HCl. To avoid this difficulty, oven dry, organic matter and $CaCO_3$ free sample weights for pipette analyses were obtained by back calculations. This method requires the precise determination of percentage H_2O, organic matter (o.m.), and $CaCO_3$ on separate samples. The percentages of these components are added together and subtracted from 100% to obtain a factor for calculating the sample weight used for particle size analysis. The equation used in the calculations is given below.

$$\text{Pipette sample weight} = \frac{100\% - (\%H_2O + \%\text{o.m.} + \%CaCO_3)}{100} \times \text{air dry sample wt.}$$

The accuracy of this method was determined to be $\pm$ 0.1 gm. by addition of the oven dry weights of the sample left in the hydrometer

jars, the 25 ml. pipette fraction, and the total sand fractions and comparing the total against the weights obtained by calculation. It was believed that less error was introduced into the analyses by obtaining sample weights in this manner than by increasing the possibility of poor dispersion. Extreme care must be taken when transferring the samples from one container to another.

Calcium Carbonate Equivalent Determinations

Calcium carbonate equivalent of the "whole soil" for each horizon was determined using the procedure outlined in U.S.D.A. Handbook No. 60 (42). (The term "whole soil" will henceforth be used to define the <2.0 mm. fraction.)

Organic Carbon Determinations

The percentage organic carbon of each soil horizon was determined by the method of Prince (35). The method was modified in that duplicate, instead of the recommended triplicate, determinations were made. Differences were noted between blanks that contained pure quartz sand and those blanks that did not. The blanks containing sand appeared to be more accurate and were henceforth used.

Determination of Free Iron Oxides of the Whole Soil

Free iron oxides were determined by the method of Kilmer (26). No modifications of this method were employed.

Determination of Cation Exchange Capacities of the Whole Soil

Cation exchange capacities of the whole soil for each horizon were determined using the procedure outlined in U.S.D.A. Handbook No. 60 (42). No modification of the method was employed. Sample weights utilized were 4.0 gm., the suggested weight for fine textured soils. The sodium concentration was determined by use of a Coleman Model 21 flame photometer.

Soil pH

The soil pH of each horizon was determined by the saturated soil paste method as outlined in U.S.D.A. Handbook No. 60 (42). Readings were made by using a Beckman Zeromatic pH meter standardized against pH 7.00 $\pm$ .01 reference buffer solution.

Bulk Density Determinations

The bulk density of selected soil horizon samples was determined by using a modified version of the "clod method" as outlined by Blake (8).

The procedure used was as follows. A natural ped ("clod") was oven dried, weighed, and attached to a thread of known weight. The ped was dipped in melted paraffin, having a temperature of approximately 60 C, and cooled. The ped, paraffin, and string were then weighed. The coated ped was then suspended in a graduated cylinder and the number of milliliters water displaced was recorded. The bulk density of the ped was calculated thusly:

$$\text{Bulk Density} = \frac{\text{Weight of oven dry ped}}{\text{Volume clod \& paraffin} - \frac{\text{Weight paraffin}}{\text{Density paraffin}}}$$

Microscopic Studies

Studies of thin sections of peds, pebbles, rocks, and heavy minerals, from selected horizons were made using a Leitz Laborluz-Pol polarizing microscope. All thin sections were made by the National Petrographic Co. of Houston, Texas, and were ground to a standard thickness of 30 microns.

The mineralogy of the soil horizons was determined by the point count method. This method entailed making traverses across the thin section and identifying each component encountered. Approximately 600 counts were made of each slide and the percentage by volume of each component calculated. Average diameter estimates of certain components in the ped thin sections were made by use of a calibrated stage micrometer. The fabric of the ped thin sections was described by using the terminology of Brewer (11). Photomicrographs were made of certain features in the thin sections by use of a Leica M2 35 mm. camera and the Leitz MIKAS micro attachment on the microscope.

Density Separation of Heavy Minerals

Heavy minerals were separated from the very fine sand fraction of selected horizons at a 2.95 s.g., using 1, 1, 2, 2 - tetrabromoethane, according to the method described by Allen (2).

A small conical test tube was poured approximately 2/3 full of the tetrabromoethane liquid. The sand fraction was added and the resulting

mixture was gently bumped on a rubber stopper to facilitate the downward movement of the heavy minerals. The contents were then centrifuged; the minerals of s.g. >2.95 were thrown to the bottom of the test tube while the minerals of <2.95 s.g. were held in suspension. The lower portion of the tetrabromoethane was frozen by placing the test tube in a small hole in dry ice. The unfrozen upper portion of the liquid was poured into a small funnel containing a coarse filter paper. The procedure was then repeated to remove the light minerals that had been entrapped and carried downward by the heavy minerals. Both the light and heavy mineral fractions were then washed with acetone, dried, and weighed. Ratios of light/heavy minerals were calculated. Magnetic components within the heavy mineral fraction were separated by use of a hand magnet and their weight percentage calculated. All fractions were saved for future analysis.

Fractionation of Sand, Silt, and Clay

The necessity of determining the different chemical and mineralogical properties of the sand, silt, and clay independently indicated the need for separating the whole soil into these fractions. The Musquiz A12, B22t, IIC1ca, and IIIC3ca horizons and the A1, B21t, and R horizons from the Kokernot soil were selected for study.

In order to facilitate the separations, the organic matter and $CaCO_3$ were removed from 100 gm. soil samples by successive H_2O_2 and HCl treatments. The samples were then washed using Buchner funnels and dispersed by shaking after the addition of 20 ml. of 5% Calgon solution.

The sand was separated by washing the sample through a 300 mesh

sieve. The sand was retained on the sieve while the silt and clay was collected in a 1000 ml. hydrometer jar. The volume of silt and clay suspension was brought to 1000 ml. and stirred. By use of Stokes law, the time required for a 2 micron particle to fall 30.5 cm. was calculated and at the end of this time, the suspension was siphoned. The distance of 30.5 cm. was arbitrary, being determined by the length of the siphoning apparatus. The hydrometer jar was again brought to volume and the procedure repeated until all clay was removed. From 12 to 21 siphonings were required for separation of the clay from the silt. The clay suspension obtained in this manner was maintained at a reasonable volume (about 500 ml.) by evaporation over a steam plate. After separation was achieved, the silt was washed from the hydrometer jar, allowed to air dry and stored for future analysis.

The total clay fraction obtained was divided into two subfractions; coarse clay (2.0 to 0.2 microns) and fine clay ($<$0.2 microns). This was done by utilizing a centrifuge to increase the settling rate. By use of a modified form of Stokes law (5) the time for a 0.2 micron particle to settle out at 2400 revolutions per minute (rpm) was calculated. The total clay fraction from each horizon was equally distributed among 8 centrifuge tubes and brought to volume at an arbitrarily selected mark. The suspensions were thoroughly mixed, and centrifuged at a 2400 rpm for the calculated time, and the supernatant suspension decanted. The procedure was repeated until separation was obtained as determined by visual inspection of the suspension after centrifugation. The number of repetitions varied among horizons, partially depending on the degree of dispersion initially obtained. The fine/coarse clay ratio was

determined by taking an aliquot of each and obtaining oven dry weights. The clay subfractions were then approximately equally divided, one portion was air dried and stored for future analyses requiring dry sample weights, and the other portion was left in suspension for X-ray diffraction analysis.

Separation of the clays from the silts and separation of the clays into subfractions resulted in large volumes of clay suspension. This volume was reduced by evaporation over a steam plate. It was noted that fungi appeared in the suspension after a period of approximately three days at the elevated temperatures. According to Stotsky and DeMumbrum (38) microorganisms in the soil may be destroyed by autoclaving for one hour at 121 C and 15 pounds/square inch with no resulting change in interplanar spacings of the clay minerals. Accordingly, the fungi infested suspensions were autoclaved three times at 2 day intervals. The fungi mycelium was then removed by passing the clay suspensions through a 300 mesh sieve. No fungi growth was detected after the series of treatments.

X-Ray Diffraction of the Silts and Clays

X-ray diffraction analyses were made on both subfractions of the total clay from the previously selected horizons.

Two methods, that of Kinter and Diamond (29) and that of Theisen and Harward (41), were initially used for orienting the clays. Preliminary tests using both these methods gave extremely poor diffraction patterns, but of the two, the method of Theisen and Harward appeared to be best suited for the clays in question. Basically, this method

was utilized throughout the X-ray diffraction analyses although several modifications were introduced.

Since the procedure of Theisen and Harward was modified, the entire procedure will be discussed. A small amount of clay suspension (volume varying with clay concentration) was poured into a 10 ml. centrifuge tube and 5 ml. of 0.3N calcium chloride ($CaCl_2$) solution were added. The suspension was mixed and allowed to stand for approximately 15 minutes. The suspension was centrifuged and the supernatant liquid poured off. The process was repeated with another increment of $CaCl_2$ solution and then washed with a 2% glycerol solution until all excess $CaCl_2$ had been removed. Two or three washings were usually adequate. The clay was stirred in the centrifuge tube by use of a glass rod, poured onto a glazed porcelain plate, smeared with the glass rod, air dried, and X-rayed.

It was noted that washing of the Ca-saturated clays with concentrations of glycerol greater than 2% resulted in poor quality patterns. Several concentrations of glycerol were tried, ranging downward from 10%.

It appeared that the concentration of glycerol required for saturation varied with the nature of the clay. Iron oxides and amorphous material were removed from the clay to see if an improvement in the patterns could be obtained. This was done by treatment with sodium hydrosulfite ($Na_2S_2O_4$) and 0.5N sodium hydroxide (NaOH) solution successively. Contrary to expectations, the treatment resulted in decreased intensity of the peaks. However, it was noted that removal of amorphous material decreased the tendency of certain coarse clays to peel.

A second plate was made using two 5 ml. increments of 0.3N potassium chloride (KCl) solution to saturate the clay and using distilled water to remove the excess KCl by centrifugation. The plate was prepared as previously described, air dried, heated at 250 C for 4 hours, and X-rayed. The same slide was then heated at 550 C for 4 hours and X-rayed again.

Certain diffractograms revealed that the clays did not completely collapse when potassium saturated and heated to 550 C. This suggested the presence of small quantities of chlorite. A method developed by Dr. C. I. Rich, Virginia Polytechnic Institute, (Personal communication from Dr. R. I. Barnhisel, University of Kentucky) to remove interlayer alumina was employed in an unsuccessful attempt to improve the resolution of the diffractograms. This treatment seemed to decrease the intensity of all reflections. It was concluded that chlorite, if present, composed a very insignificant proportion of the clay fractions.

Silt samples from each previously selected horizon were X-rayed. These samples were prepared by grinding to a fine powder and placing them in a standard metal holder for diffraction. The silts were ground primarily to insure thorough mixing of the silt particles.

The clays and silts were X-rayed with a Phillips Norelco diffraction unit using Ni filtered Cu radiation. A 1/2° divergent slit, a 0.006" receiving slit, and a 1/2° scatter slit was used in the beam collimating system. The scale factor, the multiplier, and the time constant were set at 2, 0.8, and 4, respectively, for all samples except those of the K-saturated fine clay fraction from the Kokernot R horizon. The settings for these plates were 4, 0.8, and 4. The

diffraction unit was operated at 30 kilovolts and 15 milliamperes. The plates were scanned from 2 to 32° 2θ at a rate of 1°/minute.

Differential Thermal Analyses of the Clays

Differential thermal analyses (DTA) of the clay fractions were made using a DTA pressure vacuum furnace built by Mr. William Lodding of Rutgers University. The clay samples were brought to a relative humidity of 50% by allowing them to equilibrate with a magnesium nitrate [$Mg(NO_3)_2$] slurry in a dessicator. The samples were carefully packed in the sample holder and placed in the furnace. The temperature of the furnace was automatically raised from 25 C to 1000 C at 12.5°/minute. Differences in temperature were recorded between the clay sample and an inert material of calcined aluminum oxide.

Cation Exchange Capacity Determinations of Silts and Clays

Cation exchange capacities of the silts and clays were determined using the method described in U.S.D.A. Handbook No. 60 (42). The determinations were made using oven dry 1.0 gm. samples for silts and 0.5 gm. samples for the clays. Final determinations were made with a Coleman Model 21 flame photometer.

Total Potassium Determinations of the Silts and Clays

Total potassium in the silts and clays was determined by using a slightly modified form of the method of Webber and Shivas (44). Approximately 0.2 gm. of oven dry silt and clay was accurately weighed

to 10^{-4} gm. in platinum crucibles. Exactly 1 ml. of 1:5 sulfuric acid (H_2SO_4) solution was added to the crucibles and the mixture stirred with a platinum wire. Five ml. of 40% hydroflouric acid (HF) solution was added to the mixture, the crucibles were then evaporated to dryness on a hot plate. Care was exercised to prevent splattering. By use of platinum tipped tongs, the crucibles were immersed in 150 ml. of hot 1:20 nitric acid (HNO_3) solution until the residue was dissolved. The crucibles were then removed and rinsed with distilled water. The HNO_3 solution was evaporated to dryness and the residue taken up with 0.1N HCl. The resulting solution was added to 50 ml. volumetric flasks and brought to volume with 0.1N HCl. Standard solutions of 0.0, 0.1, 0.2, 0.4, 0.6, 0.8, 1.0, 2.0, 4.0, 6.0, 8.0, and 10.0 milliequivalents (meq.), potassium (K) per liter, using KCl as the K source, in 0.1N HCl were prepared. The K content of the samples was determined by use of a Coleman Model 21 flame photometer.

Determination of Silica and Alumina of the Clays

The presence of substantial amounts of amorphous material was suspected because of the volcanic origin of the parent material, field characteristics, and some properties observed in the laboratory such as high cation exchange capacities, peeling of some coarse clay samples, and poor dispersion of some horizon samples.

Basically, Hashimoto and Jackson's (20) method of rapid dissolution was used for dissolving the amorphous aluminosilicates prior to their determination. The percentages alumina and silica were determined independently,

using the methods of McLean (34) for alumina and Kilmer (27) for silica. Some procedures were modified to varying degrees and they will therefore be outlined.

An oven dry, iron oxide free sample, weighing 0.2 gm. was placed in a nickel beaker, 100 ml. of 0.5N NaOH solution was added and the suspension boiled for exactly 2.5 minutes. The suspension was cooled to room temperature in a water bath, centrifuged, and the supernatant liquid poured into 250 ml. volumetric flasks. The samples were washed with distilled water until dispersion occurred, the washings were added to the volumetric flasks. Special care was taken to free the supernatant liquid of clay particles since a colorimetric determination was to be made. This was assured by the addition of 10 drops of 6N sodium chloride (NaCl) solution to all samples on the final washing. The 250 ml. volumetric flasks containing the supernatant liquid were brought to volume with distilled water and aliquots of the solutions were used for alumina and silica determinations.

The "aluminon" method of McLean was not altered. One ml. aliquot of the previously described supernatant solution was used.

The method of Kilmer for silica determination was slightly altered. Instead of using the recommended 10 ml. aliquot, a 2.5 ml. aliquot was drawn. The major problem encountered in this analysis was the obtaining of a standard curve. The color development of the standard as outlined by Kilmer was erratic. After several attempts, it was decided that a constant amount of reference blank solution should be added to each standard solution instead of the recommended amounts. Since 2.5 ml. aliquots were initially drawn for determination, this volume was

selected as the constant amount of reference blank solution. Preparation of the standard silicon solution in this manner resulted in a straight line curve.

CHAPTER V

DISCUSSION OF RESULTS

Particle Size Distribution

The results of the particle size distribution analyses for the Kokernot and Musquiz soils are given in Table 1. The results are averages of duplicates for all horizons. The duplicates closely agree except for those of the Musquiz IIC2 horizon. A variation of four percent occurred between duplicates of the sample from this horizon and a third analysis did not resolve the difference. Visual inspection led to the conclusion that the clay was not completely dispersed; consequently the results given for the Musquiz IIC2 horizon are questionable. It is realized that close agreement between duplicates does not mean that the results are accurate.

Table 1 also shows the volume percentage of gravel (>2mm.) of each soil horizon. These percentages will not be discussed but they are included for classification purposes.

Kokernot Soil

The clay distribution of this soil shows substantial increases with depth in the profile. This indicates that considerable clay translocation has occurred. Another possibility is that clay formation is occurring more rapidly in the lower horizons. However, the fine clay/coarse clay ratios given in Table 1 verify the former observation, assuming that fine clay is preferentially illuviated.

The silt distribution remains nearly constant throughout the

TABLE 1

PERCENTAGE OF SAND, SILT, AND CLAY BY WEIGHT, PERCENTAGE GRAVEL BY VOLUME, AND FINE CLAY/COARSE CLAY RATIOS

Soil	Horizon	Size in Mm.					
		<0.002	0.002-0.05	0.05-2.0	Gravel >2.0	Textural Class	Fine Clay / Coarse Clay
Kokernot	A1	15.6	31.5	52.9	12.6	cosl	1.6
	B1	20.0	30.2	49.8	15.4	l	
	B21t	28.7	31.0	40.3	24.4	gcl	3.1
	R/B22t	37.1	25.3	37.6	25.1	gcl	
	R						8.0
Musquiz	A12	26.6	25.6	47.8	3.0	scl	1.2
	B21t	41.7	23.3	35.0	3.1	c	
	B22t	60.2	15.3	24.5	9.3	c	7.5
	B23t	53.1	11.3	35.6	13.0	c	
	IIC1ca	28.2	23.3	48.5	17.4	scl	1.8
	IIC2	24.5	27.7	47.8	15.0	scl	
	IIIC3ca	29.3	22.2	48.5	10.6	scl	1.6
	IIIC4	14.3	47.6	38.1	4.1	l	

profile. A slight decrease in silt percentage was noted between the B21t and R/B22t horizon.

The sand distribution shows decreased percentages with depth. The decreased sand percentages correspond almost exactly with the increased clay percentages in the first three horizons. In the R/B22t horizon the increased clay percentage is offset by decreases in both the silt and sand fractions.

Musquiz Soil

The clay percentages and fine clay/coarse clay ratios indicate that substantial clay translocation has occurred in the solum. The B22t horizon is clearly the zone of maximum illuviation based on both percentage of total clay and fine clay/coarse clay ratios. The B23t, IIClca, and IIC2 horizon clay percentages are all lower than that of the B22t horizon and decrease with depth. This suggests that clay formation and translocation has decreased at the lower depths due to decreased weathering effects and that illuviation has not occurred below the B23t horizon. There is a slight increase in the clay percentage of the IIIC3ca horizon relative to the IIC2 horizon. This increase may be more apparent than real because of the problems encountered in dispersing the IIC2 horizon sample. The IIIC4 horizon clay percentage was significantly decreased relative to the overlying horizons.

The clay percentage increases are partially reflected by decreases in silt percentages with depth through the first four horizons. This coincides with expectations and is not considered significant. Examination of the silt percentages of the C horizons shows a somewhat erratic

distribution. It is believed, however, that the silt distribution remains about constant in the IIClca, IIC2, and IIIC3ca horizons. The higher percentage noted for the IIC2 horizon sample is believed to be the result of incomplete dispersion of the clay fraction. It is probable that some of the clay that did not disperse would be in aggregates of silt size. There is a very significant silt percentage increase in the IIIC4 horizon relative to the overlying horizons. This increase, coupled with the clay percentage decrease, may indicate a change in parent material or it may be the result of incomplete dispersion of the clay.

Examination of the sand distribution shows decreases in percentages with depth through the B22t horizon and an increase in sand content of the B23t horizon relative to the B22t horizon. The sand content of the first three C horizons remains approximately constant but are higher than the overlying horizons. The IIIC4 horizon sand percentage is significantly lower than the overlying C horizons.

Size Distribution of the Sand Fractions

The sand subfraction percentages based on total sand weight and the percentage of gravel (>2 mm.) based on total sample weight for the two soils are given in Table 2. The sand fraction percentages of the separates for selected horizons were plotted against size and are shown in Figures 5 and 6. Inspection of Table 2 shows that those horizon separates that were not plotted were considered to be transitional horizons between plotted horizons. They were omitted for sake of clarity of the graph. Selected sand fraction ratios were calculated and are

given in Table 3. Reference will be made to these figures and tables in the following discussion.

Kokernot Soil.

Examination of Table 2 and Figure 5 reveals that the 2.0 to 1.0 mm., very coarse sand, (vcs) fraction is dominant and has a somewhat erratic distribution in the profile. The high percentage and erratic distribution of the vcs fraction is probably the result of differential physical weathering between horizons of the parent rock and is not the result of parent material variability. The other sand fraction percentages generally show good agreement throughout the profile. Inspection of Table 3 shows that the ratios of the sand fractions remain essentially constant with depth. The sand distribution curves and tables indicate that the soil has developed from homogeneous parent material.

Musquiz Soil

The sand fraction percentages of this soil by horizon shown in Table 2 and Figure 6 reveal that the 2.0 to 1.0 mm. (vcs) and the 0.1 to 0.05 mm., very fine sand, (vfs) fraction percentages have a wide variation with depth whereas percentages of all other fractions are essentially constant. It is probable that differences in the vcs fraction percentages are due to rock fragments and are not particularly significant. However, the difference in percentage vfs, especially between the B22t and IIClca horizons, is striking. The sand fraction ratios given in Table 3 show an abrupt decrease in the IIClca horizon and a significant increase in the IIIC3ca horizon relative to the

TABLE 2

PERCENTAGE OF EACH FRACTION OF TOTAL SAND AND PERCENTAGE OF >2MM. PARTICLES OF TOTAL SAMPLE WEIGHT

Soil	Horizon	Size in Mm.					
		>2.0	2.0-1.0	1.0-0.5	0.5-0.25	0.25-0.1	0.1-0.05
Kokernot	A1	31.6	34.7	21.4	9.8	13.7	20.4
	B1	38.6	26.2	22.1	11.8	16.1	23.8
	B21t	56.1	48.4	19.3	7.3	9.5	15.8
	R/B22t	57.8	42.9	20.5	7.8	9.7	19.2
Musquiz	A12	6.9	13.5	20.3	13.3	24.1	29.0
	B21t	6.6	12.2	18.8	13.5	23.5	32.3
	B22t	23.4	23.3	17.1	10.7	20.9	28.1
	B23t	30.0	33.0	21.8	11.9	16.2	17.2
	IIC1ca	40.1	23.2	29.4	16.8	18.6	12.0
	IIC2	37.5	22.3	26.7	15.2	19.1	16.9
	IIIC3ca	25.8	34.0	22.5	11.5	15.4	16.7
	IIIC4	10.2	19.1	16.7	11.6	22.9	29.7

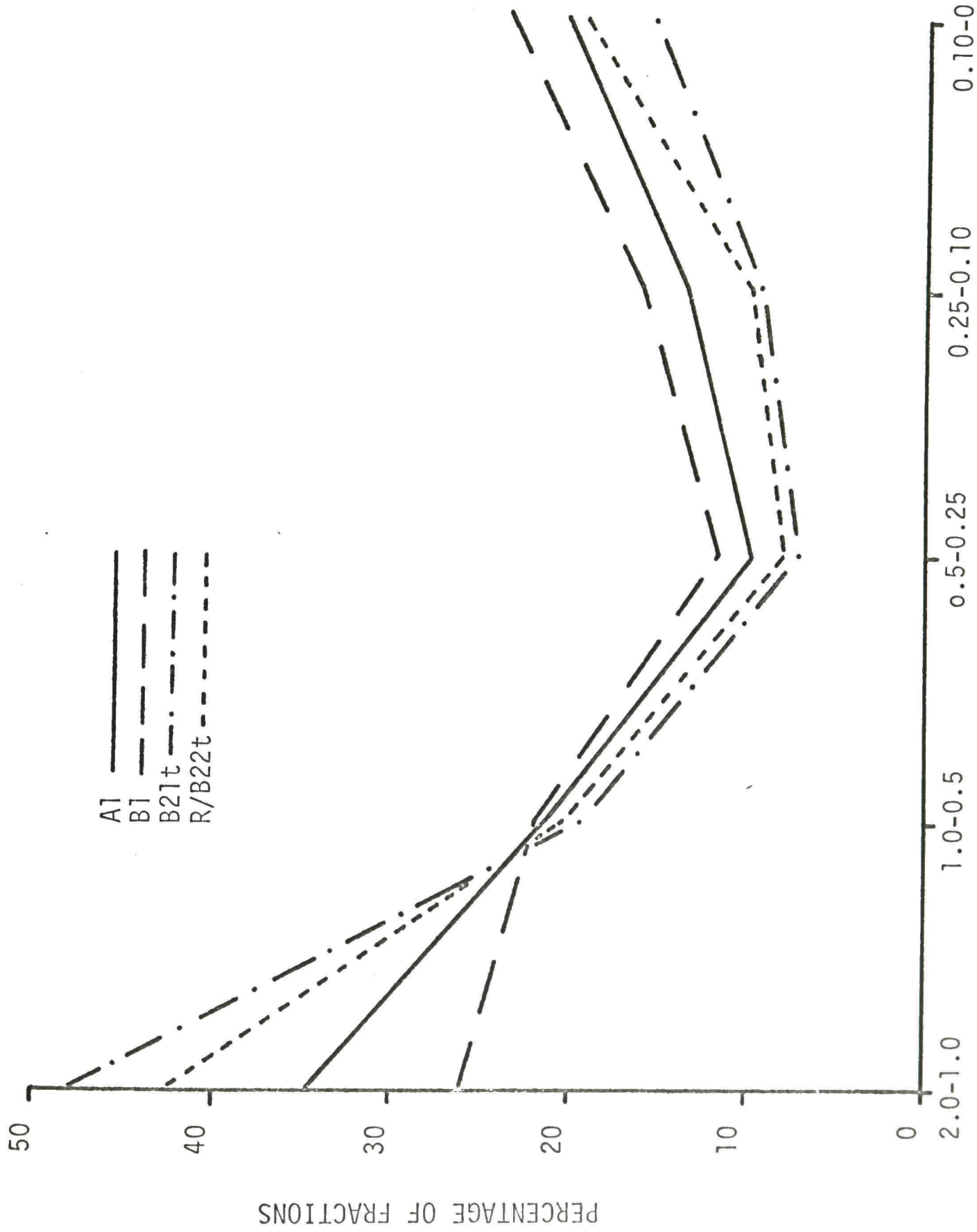

Figure 5. Particle size distribution by horizon in Kokernot soil.

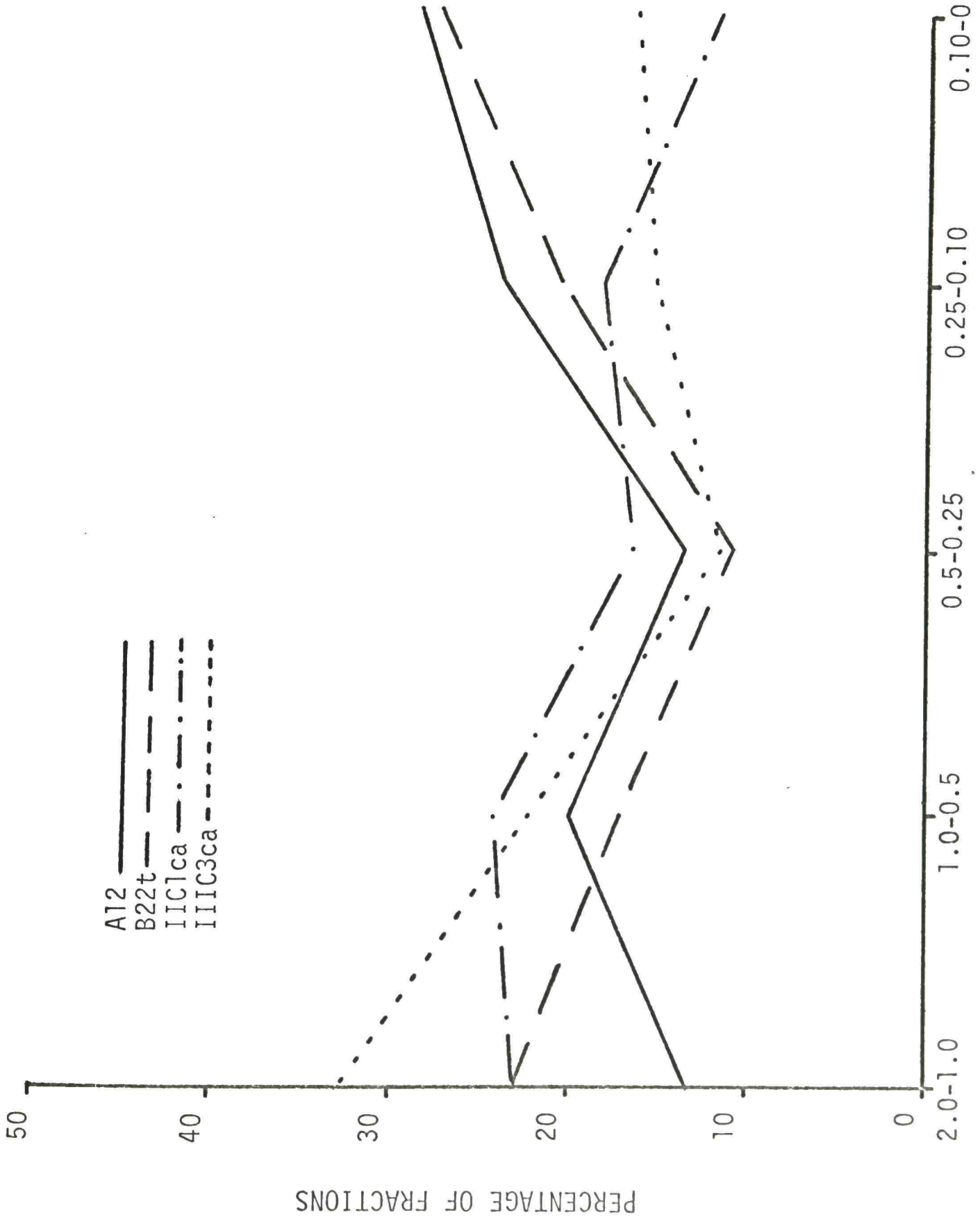

Figure 6. Particle size distribution by horizon in Musquiz soil.

TABLE 3

SELECTED SAND FRACTION RATIOS

Soil	Horizon	Fine Sand / Medium Sand	Very Fine Sand / Medium Sand	Very Fine Sand / Fine Sand
Kokernot	A1	1.40	2.08	1.49
	B1	1.36	2.02	1.48
	B21t	1.30	2.17	1.66
	R/B22t	1.24	2.46	1.98
Musquiz	A12	1.81	2.18	1.20
	B21t	1.74	2.39	1.37
	B22t	1.95	2.62	1.35
	B23t	1.37	1.45	1.06
	IIC1ca	1.11	0.71	0.65
	IIC2	1.25	1.11	0.89
	IIIC3ca	1.34	1.45	1.08
	IIIC4	1.98	2.57	1.30

overlying horizon. It is believed that the sand fraction percentages and ratios show a lithologic discontinuity between the B22t and IIClca horizons and possibly indicate another between the IIClca and IIIC3ca horizons.

Calcium Carbonate Equivalent

Kokernot Soil

There was no indication of $CaCO_3$ in this soil.

Musquiz Soil

The $CaCO_3$ equivalent for each horizon is shown in Table 4. The upper 20 inches of the profile was free of $CaCO_3$. There was a slight amount of $CaCO_3$ in the B23t horizon with the IIClca horizon being the zone of maximum accumulation. The IIC2 shows a decrease in $CaCO_3$ relative to the IIClca horizon. The percentage $CaCO_3$ of the IIIC3ca horizon is approximately equal to that noted for the IIClca horizon whereas the IIIC4 horizon was relatively free of $CaCO_3$.

The percentages $CaCO_3$ noted in the first six horizons were as expected. It is not uncommon for soils to be relatively free of carbonates in the upper horizons, have a zone of maximum accúmulation, and then show decreasing percentages in the underlying horizons. The high $CaCO_3$ percentage of the IIIC3ca horizon is somewhat unusual. It is possible that the $CaCO_3$ in the IIClca and IIIC3ca horizons was deposited under different climatic conditions. The lower accumulation in the IIIC3ca may have been deposited under somewhat more humid conditions than that of the IIClca horizon. A second, and perhaps more feasible explanation, would be that the IIIC3ca horizon developed from material which was higher in Ca bearing minerals than that material from which the overlying horizons developed. There also may have been

differential accumulation in the two horizons because of textural differences.

Organic Carbon Content

Kokernot Soil

Table 4 shows two sets of organic carbon percentages for each horizon of the soil profile. The first set of percentages, designated I, are based on the whole soil (<2 mm.) fraction; whereas, the second set of figures, designated II, are based on the whole soil plus gravel.

General inspection of the percentages shown in column I reveals an increase in organic carbon with depth through the B21t horizon and a decrease for the R/B22t horizon. The increase with depth noted in the upper horizons is believed to be more apparent than real. The percentage gravel of the Kokernot soil substantially increases with depth. This increase in gravel percentage would necessarily decrease the volume of the <2 mm. fraction and concentrate the organic carbon. Conversion of percentage organic carbon of the whole soil (<2 mm.) to percentage organic carbon of the whole soil plus gravel shows that the percentage increases slightly in the B1 relative to the A1 horizon but decreases with depth in the underlying horizons. The decrease in organic carbon coincides more closely with expectations.

Musquiz Soil

The percentage organic carbon based on the whole soil given in column I shows decreased amounts with depth in the profile. Conversion of the percentages organic carbon of the whole soil to percentage

TABLE 4

SELECTED CHEMICAL DATA FOR THE WHOLE SOILS (<2MM.)

Soil	Horizon	Percentage				CEC Meq./100gm.	Soil pH
			Organic Carbon				
		$CaCO_3$	I*	II**	Fe_2O_3		
Kokernot	A1		1.25	0.85	1.70	11.4	6.5
	B1		1.50	0.92	1.88	14.0	6.5
	B21t		1.70	0.75	1.76	19.0	6.6
	R/B22t		1.22	0.52	1.76	24.4	6.6
Musquiz	A12		1.72	1.60	2.10	16.4	6.0
	B21t		1.38	1.29	2.38	21.2	6.0
	B22t		1.19	0.91	2.74	33.9	6.5
	B23t	1.4	0.97	0.68	2.52	32.8	7.0
	IIC1ca	23.6	0.32	0.19	1.40	17.4	7.8
	IIC2	13.1	0.19	0.12	1.60	20.4	7.8
	IIIC3ca	23.5	0.16	0.12	1.32	19.0	7.8
	IIIC4	2.0	0.09	0.08	1.78	24.2	7.8

* Whole Soil (<2mm.)
** Whole Soil Plus Gravel

organic carbon of the whole soil plus gravel simply enhanced the decrease.

Free Iron Oxide Content

Table 4 gives the free iron oxide (Fe_2O_3) content for each horizon of the Kokernot and Musquiz soils. The values are averages of duplicates for all samples.

Kokernot Soil

The Fe_2O_3 content of all horizon samples remains approximately constant throughout the profile. This suggests formation in situ from the weathering of minerals contained in the parent material. Microscopic studies, to be discussed later, indicated that iron oxides were being formed during the alteration of unidentified dark minerals. The slightly higher value noted for the B1 horizon may be the result of movement of iron from the A1 horizon.

Musquiz Soil

The values in Table 4 show a gradual increase in Fe_2O_3 content through the B22t horizon and then a gradual decrease through the IIClca horizon. The quantity in the lower C horizons is somewhat erratic. The percentage Fe_2O_3 in the upper five horizons appears to coincide very closely with the clay content in those horizons. This suggests that the Fe_2O_3 has moved in association with the translocated clay. However, other work at Texas Technological College (B. L. Harris, Determination of iron in the clay fraction of four selected soils, Unpublished data) has shown that the B22t horizon fine clay has 2.35%

Fe_2O_3. Complete data on the Fe_2O_3 distribution by size fractions was not obtained.

Cation Exchange Capacity of the Whole Soil

Cation exchange capacity (CEC) results for the Musquiz and Kokernot soils are given in Table 4. The results given are the averages of duplicates for all horizons. Since X-ray diffraction analysis, to be discussed later, indicated the presence of a swelling component, illite, and kaolinite in all clay fractions, the CEC of these clay minerals will be given. Grim (18) states that the CEC ranges in milliequivalents per 100 grams (meq./100 gm.) of montmorillonite, illite, and kaolinite are 80 to 150, 10 to 40, and 3 to 15 meq./100 gm., respectively.

Kokernot Soil

The CEC of each horizon is closely correlated with its clay content. Both the clay content and CEC of the horizons increase with depth. Conversion of the clay percentages to a 100 gm. clay basis shows that the CEC decreases from a high of 73 meq./100 gm. in the A1 horizon to a low of 66 meq./100 gm. in the R/B22t horizon. This indicates that the clay fraction must contain a considerable amount of a swelling type clay, or amorphous material, or both. Assuming that the swelling component has a CEC of 100 meq./100 gm., it would have to be present in the clay fraction in amounts $\geq$50%. If the swelling component composed only 50% of the total clay fraction then the illite/kaolinite ratio would be large. Increased amounts of the swelling component would lower the illite/kaolinite ratio.

The silt and organic matter fractions, no doubt, contribute to

the CEC of each horizon and would tend to slightly lower the clay CEC value estimates.

Musquiz Soil

The CEC of all horizons except the IIC2 and IIIC4 horizons correspond very closely to their respective clay percentages. When the clay percentages are converted to a 100 gm. clay basis the CEC ranges from 51 meq./100 gm. in the B21t horizon to 64 meq./100 gm. in the IIIC3ca horizon. This indicates that a swelling type clay must be present in quantities of not less than 30% of the total clay fraction. When the clay percentages of the IIC2 and IIIC4 horizons are converted to a 100 gm. clay basis, the CEC's are 92 and 169 meq./100 gm., respectively. These values are abnormally high and are, no doubt, the result of incomplete dispersion of the samples, causing low clay percentages, during particle size analysis. The CEC of the whole soil fraction of the IIC2 and IIIC4 horizon samples are also higher than the overlying and underlying horizons. This also indicates that the clay content of these horizons is higher than was shown by particle size analysis. The reason for poor dispersion of the samples from these horizons is not apparent. It is possible that the higher CEC's are caused by the presence of amorphous material which, in turn, acts as a binding agent to form clay aggregates and prevents dispersion.

Soil pH

The pH of each horizon of the Kokernot and Musquiz soils was determined in duplicate and averages of the results are given in Table 4.

The values for both soils are lower than would be expected for soils developed under an average annual rainfall of less than 20 inches. This is especially true for the Musquiz soil since the lower horizons are known to contain free $CaCO_3$. The reason for the low pH values is not apparent. The values may reflect to some extent the mineralogy of the clay fractions. Clay minerals with 2:1 lattices would tend to hold divalent cations more tightly than monovalent hydrogen ions. The disassociated hydrogen ions might account for the lower pH values. Data on percentage base saturation would perhaps shed light on the situation.

Bulk Density

The bulk densities of natural peds taken from selected horizons was determined and are given in Table 5. The values are an average of duplicates or, in some cases, triplicates. The values for both soils are not considered to be unusual except for the Kokernot A1 horizon. The bulk density of this horizon is considerably higher than was expected. The presence of appreciable quantities of gravel (s.g. of about 2.5) in both soils no doubt affects the bulk density measurements and care should be exercised in drawing conclusions based on the values.

Microscopic Studies

Kokernot Soil

Thin sections of peds from the B1, B21t, and R/B22t horizons and of rock taken from the R/B22t and R horizons were studied. The B1 and

TABLE 5

BULK DENSITY (gm./cm.^{3})

Soil	Horizon	Bulk Density
Kokernot	A1	1.81
	B21t	1.43
	R/B22t	1.49
Musquiz	A12	1.56
	B22t	1.64
	IIC1ca	1.41
	IIIC3ca	1.38

B21t horizon thin sections were horizontally cut; all other were randomly cut. Descriptions of the physical and mineralogical properties are given below. The average diameters of the components are also given but because of extreme particle size variability, they are, at best, estimates.

The term "groundmass" is employed in describing the mineralogy of both the ped and rock thin sections and its use is defined in the description of the R horizon thin section. The groundmass was composed mostly of microperthite.

B1 Horizon (Ped)

Mineralogy.

Components	Percentage	Average Diameter (mm.)
Groundmass Fragments	29	3.00
Feldspar (Sanidine)	10	0.21
Quartz	3	0.11
Iron Oxide Segregations and Unidentified Dark Minerals	2	0.12
Matrix	39	

Color. The color description of the components under plane polarized light follows. The quartz was colorless. The feldspar was colorless to dark gray. The groundmass fragments were splotchy gray to light brown in color. The brown color of the groundmass was often enhanced by iron oxide stains. The altered unidentified mafic minerals were dark brown to black. The iron oxide segregations appeared metallic gray to submetallic orange under reflected light.

Voids. The voids were dominantly irregular, prolate, simple

packing types having a 0.25 mm. average diameter. They occupied approximately 15% of the slide area and were occasionally partially filled with plant root remains.

Cutans.

a. Color. Light brown.

b. Surfaces Affected. Embedded grains.

c. Mineralogical Nature. Classified as ferri-argillans; a mixture of silicate clays and iron oxides.

d. Fabric. Diffusion cutans. Boundaries were rather diffuse with weak orientation.

e. Size. Average of 8 microns. Composed 1% of the thin section.

General Features. The matrix material, defined as the fine grain material, was composed of silicate clays, minute iron oxide particles, and unidentified silt size mineral grains; it exhibited no noticeable orientation of the silicate clays. The angular quartz particles did not exhibit evidence of weathering. The feldspar, predominantly sanidine, was slightly weathered around the edges and along cleavage planes. A single plagioclase particle was identified. Occasional small zircon particles were identified but did not fall along the counting traverse.

B21t Horizon (Ped)

Mineralogy.

Components	Percentage	Average Diameter (mm.)
Groundmass Fragments	25	No estimate
Feldspar (Sanidine)	12	0.28
Quartz	2	0.10
Iron Oxide Segregations and Unidentified Dark Minerals	3	0.13
Matrix	35	

Color. Under plane light, the matrix material was light brown to yellowish brown. The colors of the other constituents were the same as those described for the B1 horizon. Characteristic colors of the different constituents under plane light are shown in Figure 7.

Voids. Voids composed 21% of the thin section area and were of the same type as described for the B1 horizon.

Cutans.

a. Color. Yellowish brown to reddish brown.

b. Surfaces Affected. Dominantly embedded grain cutans. A few free grain cutans.

c. Mineralogical Nature. The same as that described for the B1 horizon.

d. Fabric. Dominantly diffusion cutans. Occasional discontinuous, illuviation cutans. Rather diffuse boundaries and moderate orientation.

e. Size. Average 16 microns. Upper range of 0.06 mm. thickness. Composed 2% of the section area.

General Features. The matrix material was composed of the same constituents as described for the B1 horizon. The matrix appeared to have very slight orientation of the silicate clays. Angular quartz particles exhibited no noticeable weathering effects. Feldspars, in general, were moderately weathered around edges and along cleavage planes but a few appeared to be extensively weathered, especially along the outer edges of the ped. These features, as well as the general nature of the groundmass fragments and cutans, are shown in Figures 8 and 9.

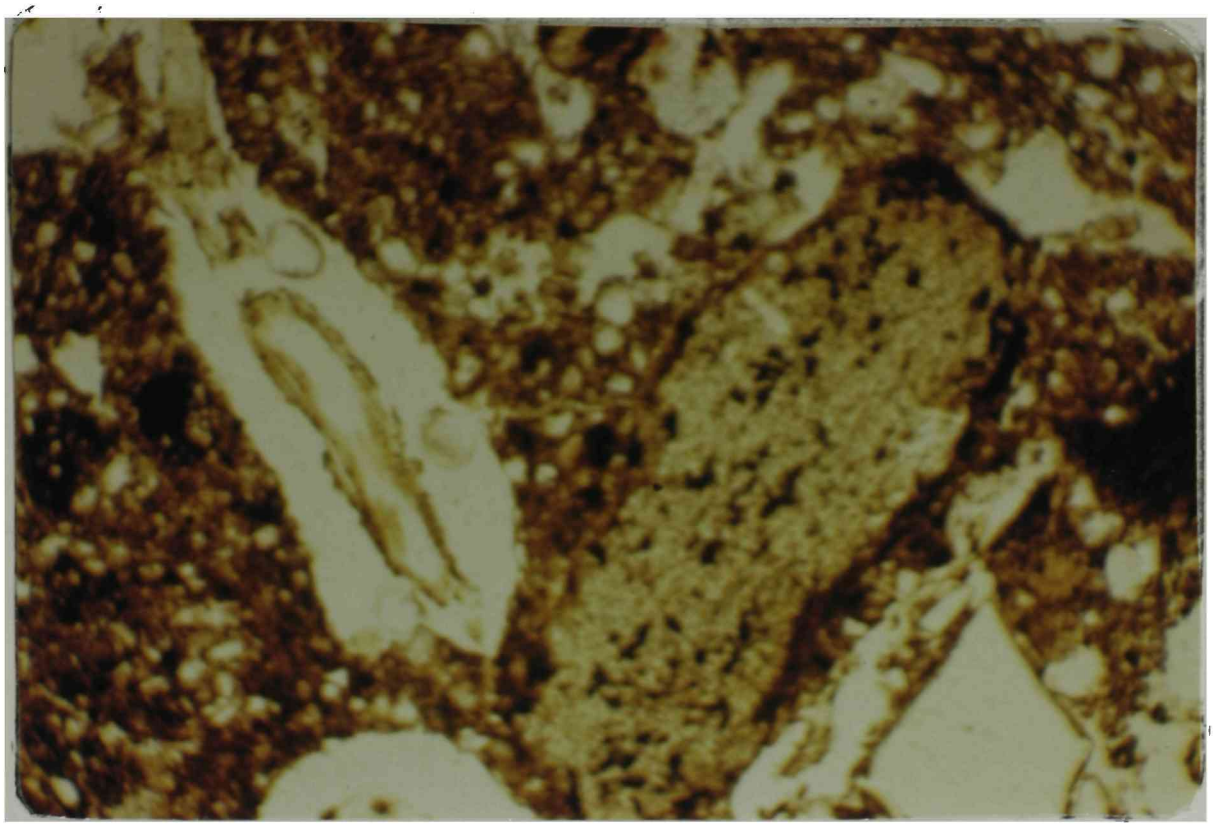

Figure 7.--Color and general fabric of a ped from the B21t horizon. Plane polarized light and 24X magnification.

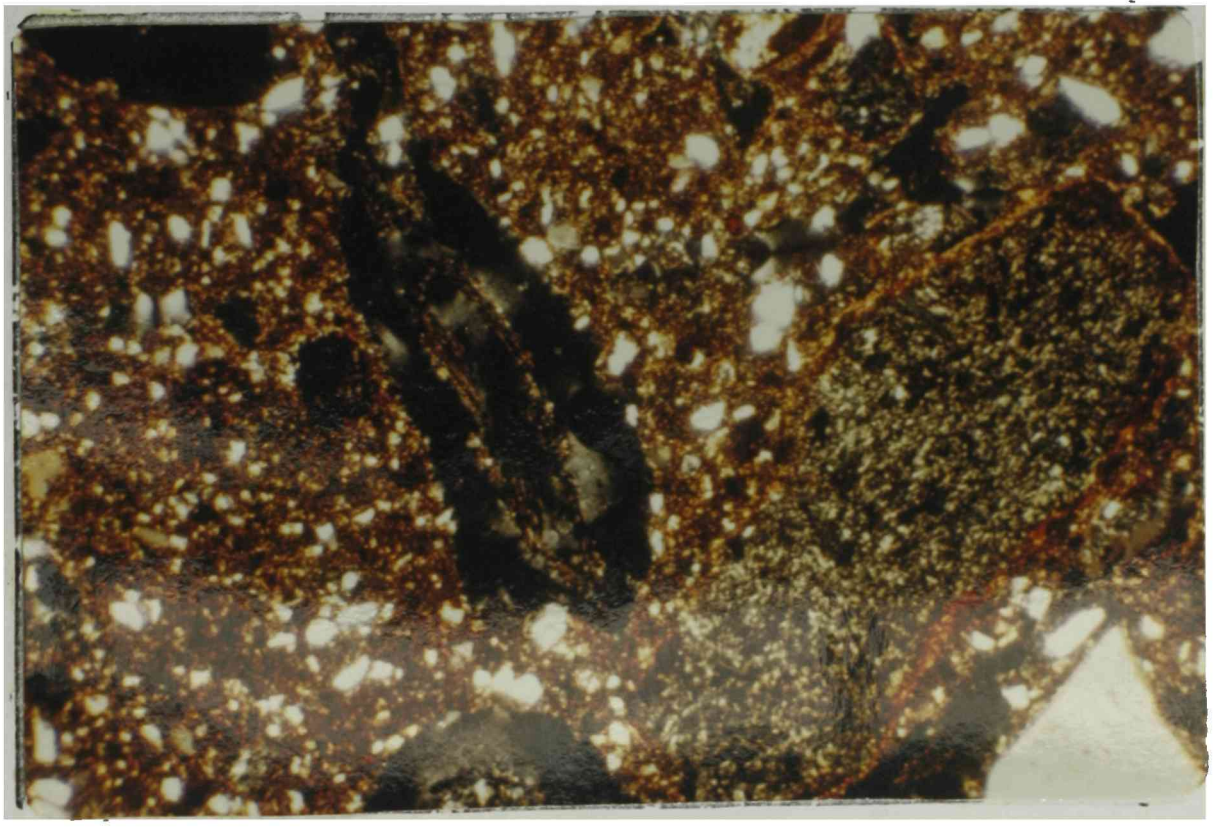

Figure 8.--General features of a B21t horizon ped. Moving from center to lower right, a void with root remains, a groundmass fragment, and a feldspar particle are evident. Crossed polarizers and 24X magnification.

Occasional glass fragments and highly birefringent zircon particles were noted. Normal void cutans were notably lacking in the section.

R/B22t Horizon (Ped)

Mineralogy.

Components	Percentage	Average Diameter (mm.)
Groundmass Fragments	48	No estimate
Feldspar (Sanidine)	5	0.26
Quartz	<1	0.09
Iron Oxide Segregations and Unidentified Dark Minerals	2	0.15
Matrix	21	

Color. Mineral colors were generally unchanged from those described for the B21t horizon.

Voids. Voids, composing 14% of the area, were principally continuous irregular, branching channels which had an average width of 0.22 mm. Infrequent normal packing voids were noted.

Cutans.

a. Color. Very dark brown to yellowish brown.

b. Surfaces Affected. Dominantly free grain and channel void cutans. Few embedded grain cutans.

c. Mineralogical Nature. Classified as ferri-argillans; a mixture of silicate clays and iron oxides.

d. Fabric. Almost entirely illuviation cutans. Some embedded grain diffusion cutans. Rather sharp boundaries and strong continuous orientation.

e. Size. Range of 8 microns to 0.48 mm. Composed 10% of the slide area.

General Features. The matrix was composed of silicate clay, minute iron oxide particles, and unidentified mineral grains, mostly of silt size. It appeared that the silt size mineral grains were often concentrated in some areas of the matrix but other areas contained only a limited number of grains. No patterns of concentration were discernible. The silicate clay of the matrix was moderately oriented. Angular quartz grains exhibited no apparent weathering. Chemical weathering of the sanidine feldspar was confined to cleavage planes and particle edges. A single zircon particle was observed but did not fall along the counting traverse. The cutan thickness was so variable that an accurate average thickness estimate was virtually impossible to make. The cutans appeared to contain increased quantities of iron oxides relative to the cutans in the previously described thin sections. A photomicrograph characteristic of the thin section is shown in Figure 10.

R/B22t Horizon (Rock)

The thin section was classified as a trachyte porphyry. Groundmass accounted for 56% of the slide area. Large euhedral sanidine phenocrysts were identified on the basis of small 2V (<34°) angles The phenocrysts composed 35% of the mineral fraction and had an average diameter somewhat greater than 1.0 mm. Mafic mineral phenocrysts were so thoroughly altered that the original minerals could not

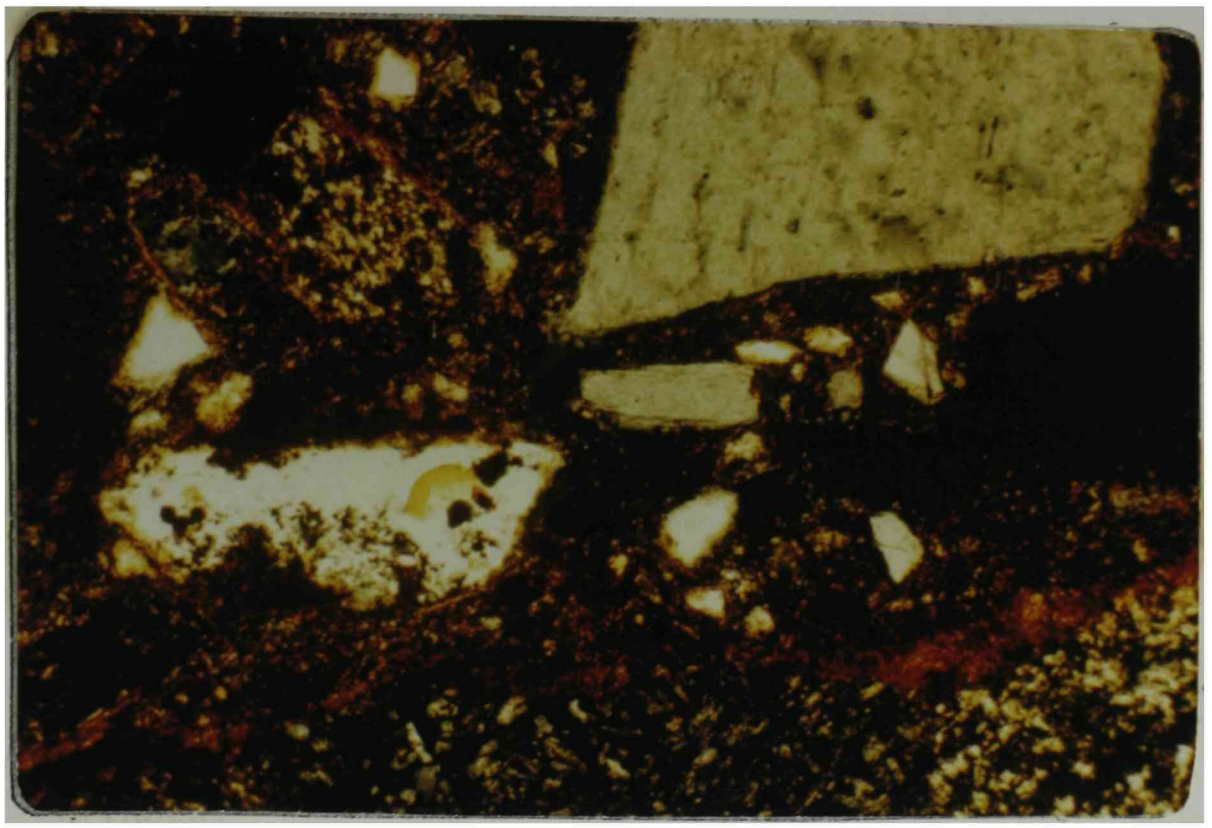

Figure 9.--General features of a ped from the B21t horizon under crossed polarizers and 80X magnification.

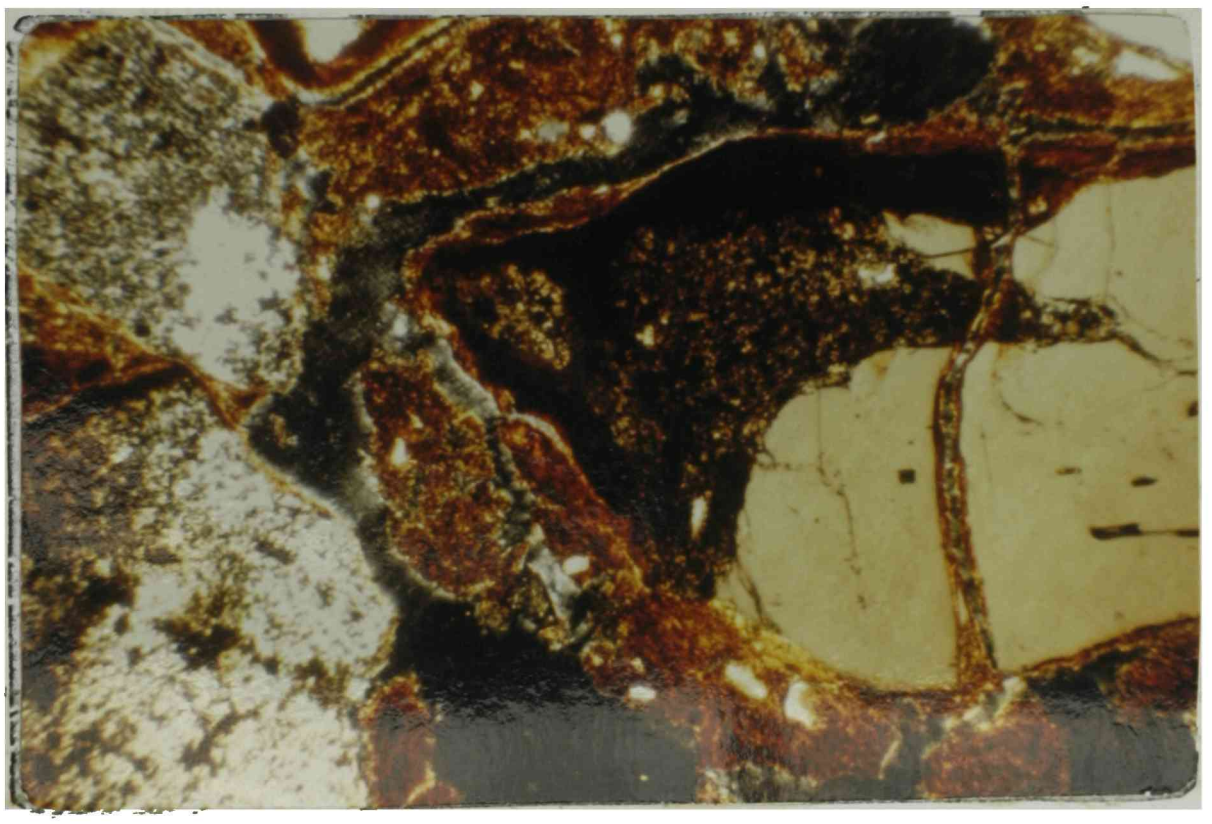

Figure 10.--General features of a ped from the R/B22t horizon. Groundmass fragment, cutan development, and feldspar particle (left to right) are shown. Crossed polarizers and 24X magnification.

be identified. The only identifiable alteration products of the mafic minerals were iron oxides. The remaining area was composed of illuviated clay, voids, quartz, and altered unidentifiable dark minerals. The percentages of these constituents was 6%, 2%, 1%, and <1%, respectively.

The groundmass and phenocrysts were not extensively weathered but exhibited numerous fracture channels. Evidence of weathering, when present, was mostly confined to exposed edges of the constituents. The fracture channels were almost entirely filled with illuviated clay.

R Horizon (Rock)

The rock of this thin section was classified as a trachyte porphyry. The groundmass was aphanitic and was composed mostly of material tentatively identified as "microperthite". No plagioclase was identified in the microperthite but it was believed to be such because of the structure and texture of the material. Also, plagioclase was identified in the silts by X-ray analysis to be discussed later. The microperthite is probably composed mostly of sanidine, but because of the small size of the particles, optical properties could not be obtained. Sections of the groundmass were optically continuous but had irregular outlines. The feldspathic portion of the groundmass exhibited considerable alteration and the scattered mafic minerals of the groundmass were unidentifiable due to alteration. Groundmass dominated the section and accounted for 66% of the area. Phenocrysts of euhedral sanidine with a 1.0 mm. average diameter composed 25% of the total mineral fraction. Mafic mineral phenocrysts were the same as those described in the R/B22t rock thin section. Voids and illuviated

clay composed 3% and 4%, respectively, of the thin section. The remaining 2.0% of the mineral fraction consisted of weathered unidentified dark minerals.

The groundmass and phenocrysts were relatively unweathered but were frequently fractured. The fracture channels were partially filled with illuviated clay. Aggregates and specks of iron oxides were disseminated throughout the section. Occasional zircon particles were noted but did not fall along the counting traverse.

General Discussion of the Kokernot Thin Sections

The thin sections from this soil gave no evidence of parent material variability. The soil apparently developed from a trachyte porphyry having a groundmass of microperthite texture. The sanidine, quartz, dark minerals, and iron oxides which were noted in all horizons were either released by physical weathering or were alteration products of the bedrock. This observation was based on the fact that an inverse relationship existed between the percentage groundmass fragments and the percentages of other minerals. The increase in feldspar/quartz ratios with depth pointed out the greater susceptibility to weathering of feldspar.

The cutans, classified as ferri-argillans, were dominantly diffusion cutans in the upper horizons and were dominantly illuviation cutans in the lower horizons. Their percentage increased with depth to the R horizon which indicates that considerable water has moved throughout the profile.

Musquiz Soil

Thin section studies were made on peds and pebbles taken from selected horizons of the Musquiz soil. One ped from each of the B horizons was horizontally cut and another ped from the B22t horizon was vertically cut. A IIClca horizon ped was randomly cut. Four thin sections, randomly cut, were made of pebbles taken from the B21t and IIIC3ca horizons. Descriptions of the physical and mineralogical properties and average diameter estimates are given below.

In the discussion that follows, the terms "Groundmass fragment, type 1" (GM-1) and "Groundmass fragment, type 2" (GM-2) will be used in describing the ped thin sections. The type 1 fragments had mostly a microperthite texture and were probably derived from trachytic type rocks. The type 2 fragments had microgranular, granophyric, and felted textures. These fragments were derived from rhyolitic and perhaps other trachytic rocks. Type 1 fragments were predominantly composed of feldspar. Altered mafic minerals were sometimes present. Type 2 fragments contained appreciably more quartz than type 1 fragments.

B21t Horizon (Ped)

Mineralogy.

Component	Percentage	Average Diameter (mm.)
Groundmass Fragments (type 1)	12	No estimate
Groundmass Fragments (type 2)	<1	No estimate
Feldspar (Sanidine)	9	0.20
Quartz	4	0.08
Iron Oxide Segregations and Unidentified Dark Minerals	2	0.08
Matrix	54	

Color. Colors of the minerals under plane polarized light may be described as follows. Quartz was colorless and feldspar was colorless to gray, depending on the degree of weathering. Both types of groundmass fragments gave a splotchy gray color and the matrix was reddish brown. Iron oxide segregations and unidentified dark minerals were brown to black. Under reflected light they appeared metallic gray to submetallic orange.

Voids. The voids were irregular, prolate, simple packing types that accounted for 17% of the slide area. Average diameter of the voids was 0.26 mm.

Cutans.

a. Color. Varied from light to dark reddish brown.

b. Surfaces Affected. Dominantly embedded grain cutans but some free grain and normal void cutans.

c. Mineralogical Nature. A mixture of silicate clay and iron oxides. Classified as ferri-argillans.

d. Fabric. Principally diffusion cutans. Boundáries rather diffuse with moderate orientation. A few scattered illuviation cutans noted.

e. Size. Average of 12 microns. Composed 2.0% of the slide area.

General Features. The matrix was composed of silicate clays, minute iron oxide particles, and unidentifiable mineral grains mostly of silt size. There appeared to be a slight degree of orientation in some small areas of the matrix. The oriented areas seemed to be surrounding

silt particles. In general, the quartz grains showed little effect of weathering. Feldspars exhibited various weathering stages, ranging from slight to extensive. Occasional plagioclase feldspar particles were noted but did not fall along the counting traverse. The size range of the GM-1 and GM-2 fragments was extremely variable so an average diameter was not determined.

B22t Horizon (Ped - Horizontal Cut)

Mineralogy.

Component	Percentage	Average Diameter (mm)
Groundmass Fragments (type 1)	8	No estimate
Groundmass Fragments (type 2)	3	No estimate
Feldspar (Sanidine)	4	0.20
Quartz	3	0.09
Iron Oxide Segregations and Unidentified Dark Minerals	1	0.10
Matrix	56	0.08
Zircon	<1	

Color. The colors of the constituents were the same as noted for the B21t horizon. Figure 11 shows the color of the matrix and iron oxide segregations under reflected light.

Voids. Voids accounted for 11% of the section and were the same type as described for the B21t horizon. Average diameter was 0.25 mm.

Cutans.

a. Color. Yellowish brown to reddish brown.

b. Surfaces Affected. Dominantly embedded grain and normal void cutans. Few free grain cutans.

c. Mineralogical Nature. Similar to that described for the B21t horizon.

d. Fabric. Rather sharp boundaries with moderate orientation. Embedded grain cutans were principally diffusion cutans; whereas, normal voids had principally illuviation cutans.

e. Size. Average of 20 microns. Range of 8 microns to 0.08 mm. thick. Accounted for 14% of the section.

General Features. The matrix was of the same nature as that described for the B21t horizon. The matrix exhibited moderate orientation. The general fabric of the thin section is shown in Figure 12.

Most of the quartz particles were angular in shape and showed little weathering effect. Feldspars exhibited all stages of weathering and most were weathered around the edges and along cleavage planes. Several feldspar particles of 0.8 mm. size were noted but their occurrence did not alter the average diameter estimate to a great extent.

B22t Horizon (Ped - Vertical Cut)

Mineralogy.

Component	Percentage	Average Diameter (mm.)
Groundmass Fragments (type 1)	9	No estimate
Groundmass Fragments (type 2)	2	No estimate
Feldspar (Sanidine)	4	0.22
Quartz	3	0.10
Iron Oxide Segregations and Unidentified Dark Minerals	1	0.11
Matrix	65	

Color. The colors of all minerals were unchanged from those noted

in the description of the horizontally cut ped.

Voids. Voids were the same type as those described for the horizontally cut ped and accounted for 8% of the thin section. Average diameter of the voids was 0.18 mm.

Cutans.

a. Color. Yellowish brown to reddish brown.

b. Surfaces Affected. Dominantly embedded grain and normal void cutans. Occasional free grain cutans.

c. Mineralogical Nature. Similar to that described for the horizontally cut ped.

d. Fabric. Rather diffuse boundaries with moderate orientation. Diffusion and illuviation cutans present.

e. Size. Average of 25 microns. Range of 8 microns to 0.10 mm. Cutans composed 8% of the slide area.

General Features. In general, the features of this thin section were identical to those of the horizontally cut ped. However, the matrix material exhibited stronger orientation and the cutan percentage was significantly lower (See Figure 13). Figures 12 and 13 show the contrast in orientation of cutans between the horizontally and vertically cut peds.

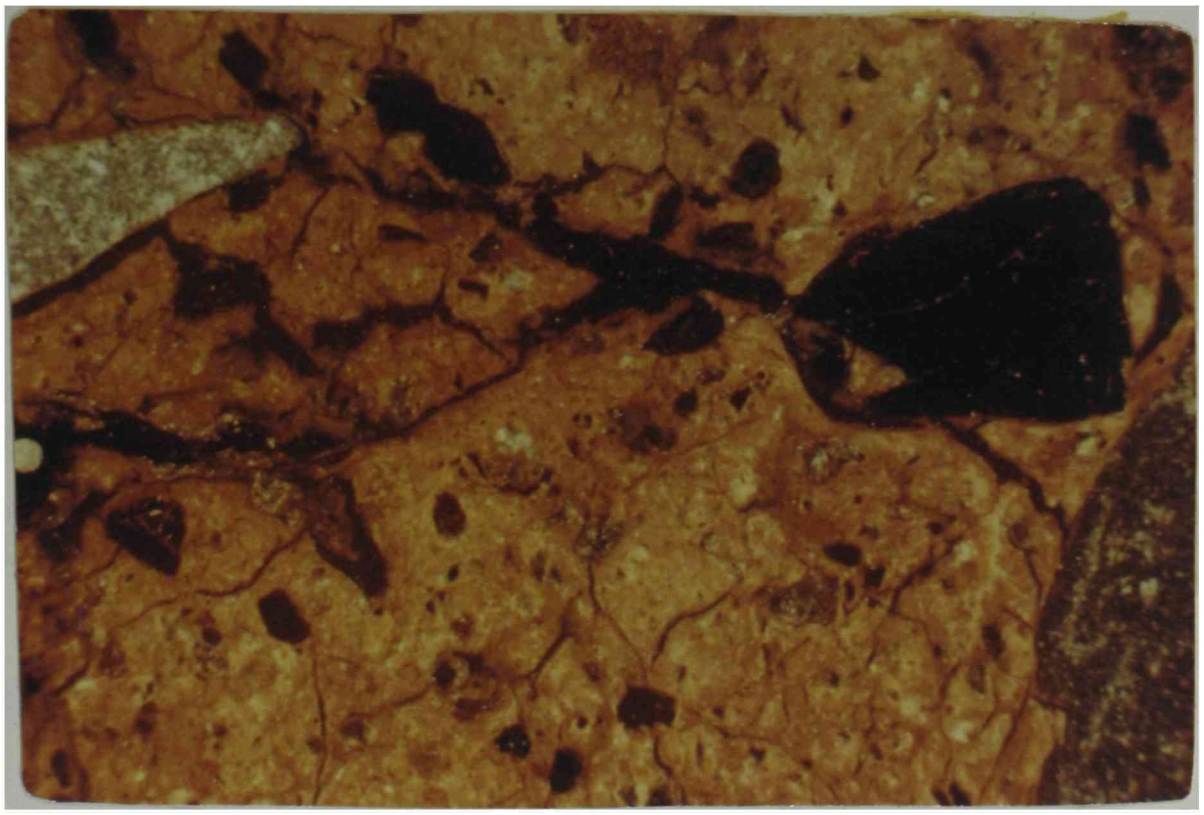

Figure 11.--Color and general appearance of matrix and iron oxide segregations of a ped from the B22t horizon. Reflected light and 24X magnification.

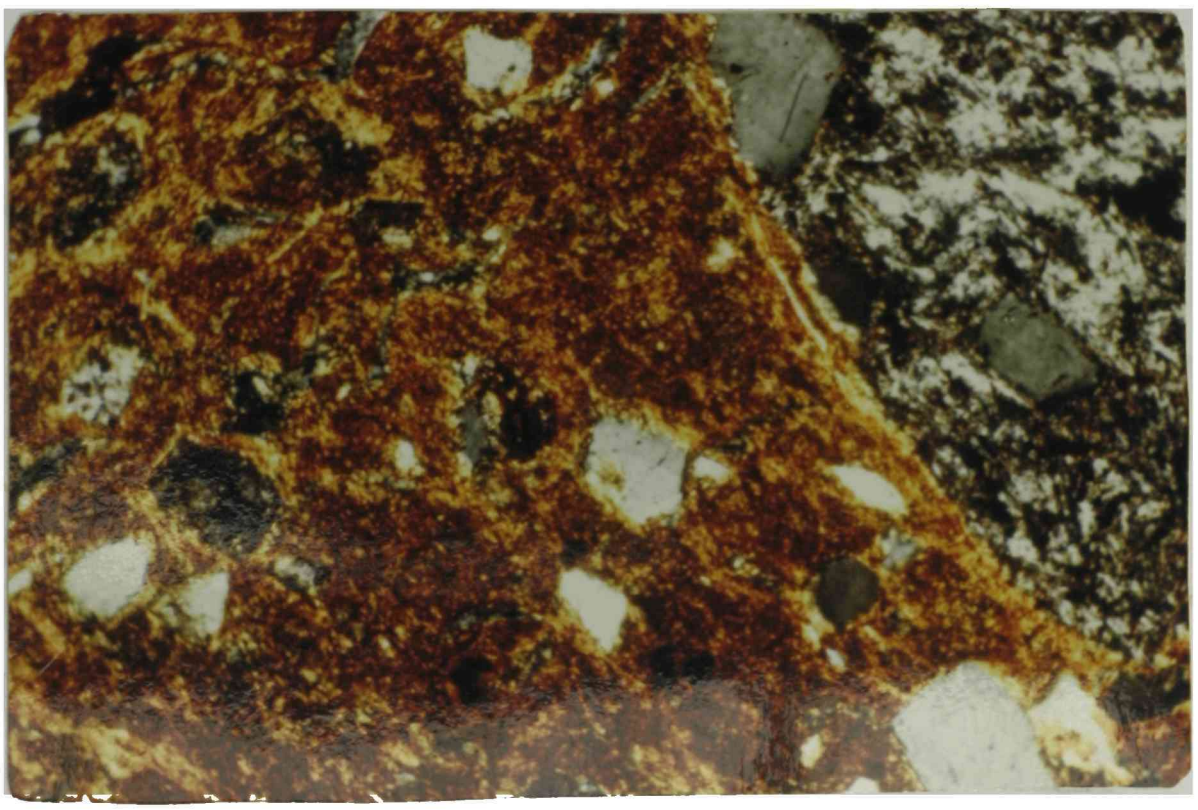

Figure 12.--General fabric of a horizonatlly cut ped from the B22t horizon. Crossed polarizers and 80X magnification.

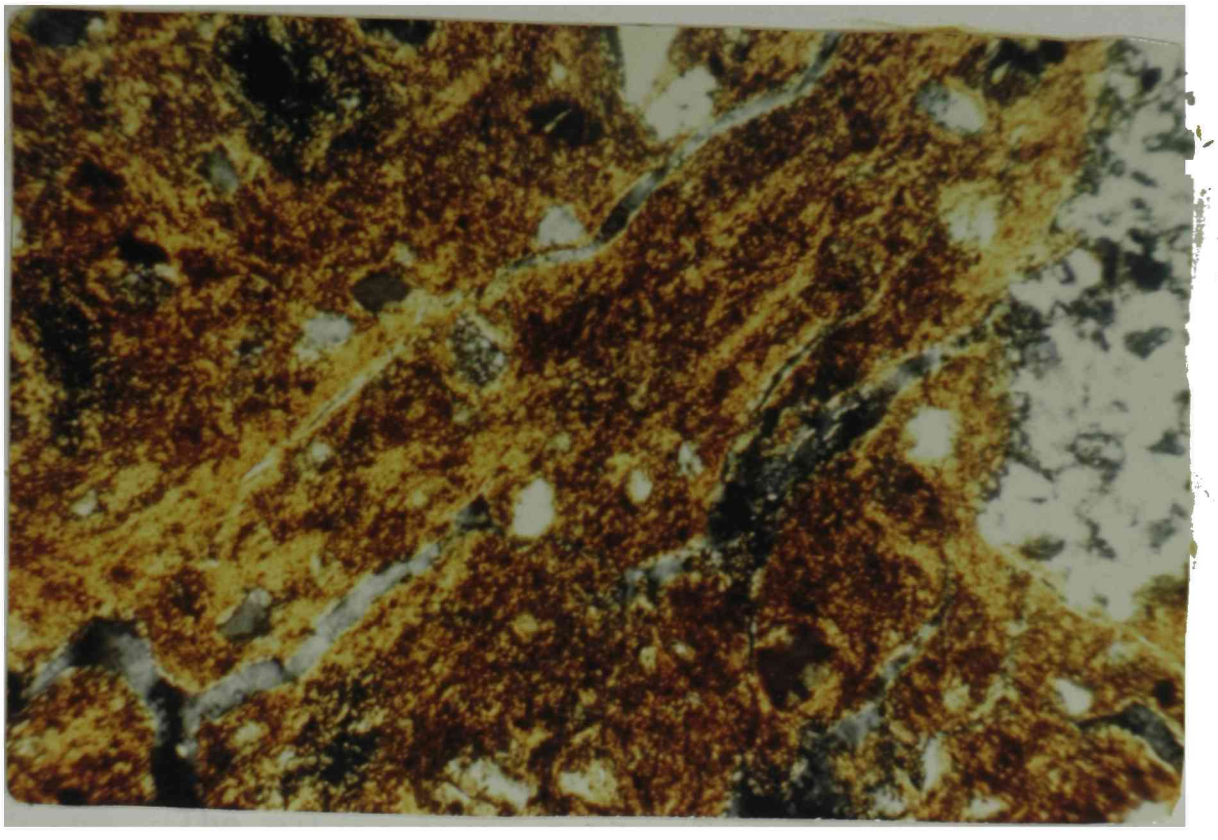

Figure 13.--General fabric of a vertically cut ped from the B22t horizon. Crossed polarizers and 80X magnification.

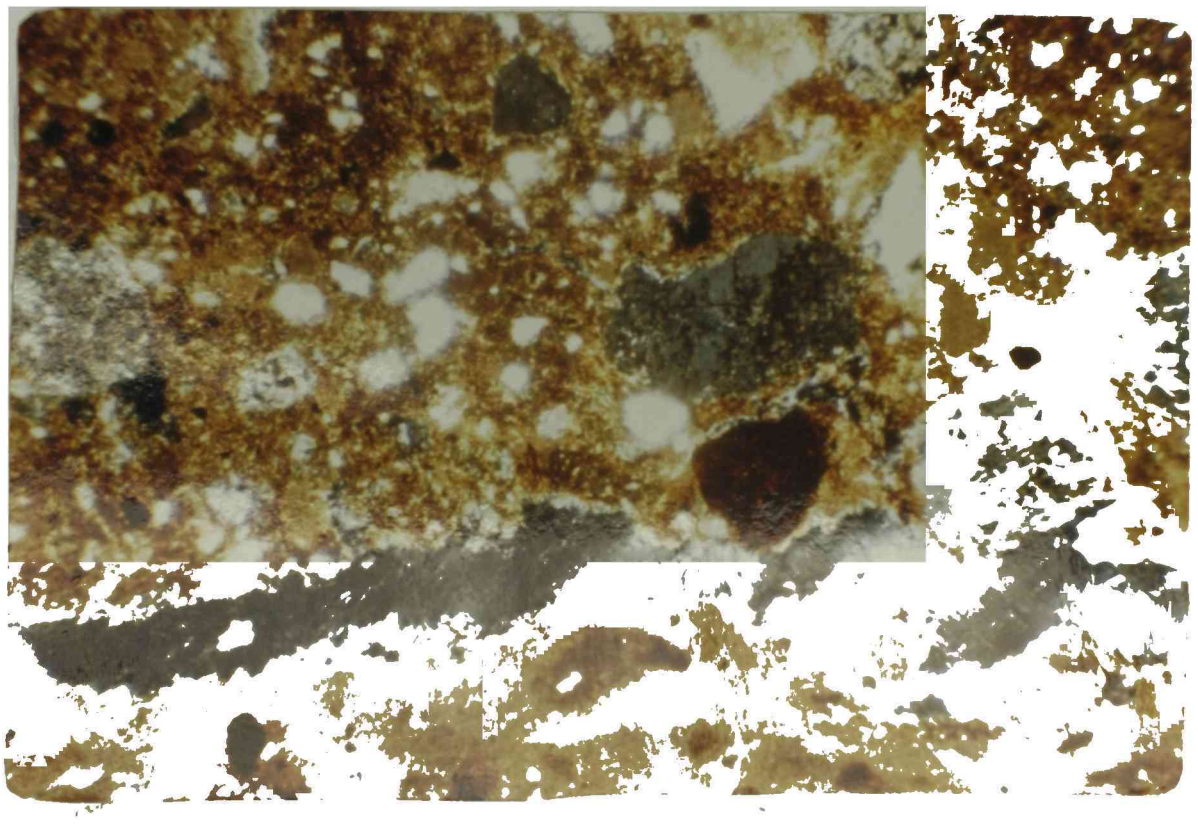

Figure 14.--General fabric of a ped from the IIClca horizon. The boundary between the part strongly impregnated with $CaCO_3$ (lower one-third) and the weakly impregnated part (upper two-thirds) is apparent. Crossed polarizers and 24X magnification.

B23t Horizon (Ped)

Mineralogy.

Component	Percentage	Average Diameter (mm.)
Groundmass Fragments (type 1)	30	No estimate
Groundmass Fragments (type 2)	7	No estimate
Feldspar (Sanidine)	8	0.24
Quartz	4	0.11
Iron Oxide Segregations and Unidentified Dark Minerals	3	0.11
Matrix	28	

Color. The matrix material was reddish brown in color. The GM-1 and GM-2 colors appeared very light brown instead of cloudy gray as previously noted. All other constituents had colors similar to those described for the B21t horizon peds.

Voids. The voids were classified as irregular, prolate, simple packing types with an average diameter of 0.24 mm. These voids composed 9% of the thin section.

Cutans.

a. Color. Yellowish brown to reddish brown.

b. Surfaces Affected. Approximately equal proportions of free grain, embedded grain, and normal void cutans.

c. Mineralogical Nature. Similar to that described for the B21t horizon.

d. Fabric. Rather diffuse boundaries with moderate orientation. Approximately equal amounts of illuviation and diffusion cutans.

e. Size. Average 16 microns. Composed 11% of the thin section.

General Features. Most of the oriented areas in the matrix appeared to be surrounding silt size particles. The angular quartz particles appeared unweathered. In general, the feldspars were weathered only around the particle edges and along cleavage planes. A few large feldspar particles, >1.5 mm. diameter, were observed. A single small grain of plagioclase feldspar was identified. The groundmass fragments, generally of very large size, did not appear to be significantly weathered. Occasional highly altered fragments, mostly of glass, were noted. These bands of fragments had a light orange color under reflected light. Three zircon particles were identified but did not fall along the counting traverse.

IIClca Horizon (Ped)

This ped was selected for sectioning so that a boundary between a part strongly impregnated with $CaCO_3$ and a part containing only diffuse patches of $CaCO_3$ was included. The two distinct parts of the ped shown in Figure 14, will be described separately. No attempt was made to distinguish between the types of groundmass fragments or to estimate diameters of the constituents.

Mineralogy of Weakly Impregnated Part.

Component	Percentage
Groundmass Fragments	26
Feldspar	7
Quartz	3
Iron Oxide Segregations and Altered Dark Minerals	2
Matrix	37
Calcite	15
Cutans	1
Voids	8

General Features. Under plane light the matrix material was light reddish brown and no evidence of orientation could be detected. The feldspar and quartz particles were generally colorless. Weathering of feldspars along cleavage planes showed up as dark gray areas. The groundmass fragments were splotchy gray to light brown. Calcite was light brown to gray. Voids were generally irregular, prolate, simple packing types but some channel voids occurred. Cutans were yellowish brown in color and had an average thickness of 8 microns. The cutans were principally weakly oriented diffusion cutans and had rather diffuse boundaries. Some free grain illuviation cutans were noted. Occasional plagioclase and zircon particles were identified.

Mineralogy of Strongly Impregnated Part.

Component	Percentage
Groundmass Fragments	7
Feldspar	3
Quartz	1
Iron Oxide Segregations and Altered Dark Minerals	2
Calcite	80
Voids	8

General Features. The general color of this part of the section under plane light was light brown. Quartz, feldspar, and groundmass appeared the same as they did in the weakly impregnated part of the section. It appeared that voids were often formed by solution of the calcite away from embedded grains. Iron oxide segregations and altered dark minerals were black under plane light but appeared metallic gray to submetallic orange under reflected light. Matrix material was so

highly impregnated with calcite that differentiation between the two was impossible. Cutans apparently did not develop because of the calcite.

Pebble Thin Sections

Thin sections were made of four representative pebbles selected from the Musquiz soil in order to partially characterize the lithology of the parent material. Two pebbles were taken from the B2t horizons and two from the IIIC3ca horizon.

All of the pebbles were classed as porphyritic trachytes or porphyritic rhyolites. The groundmass was holocrystalline and aphanitic in each case. The B2t-no.1 pebble groundmass had such a fine texture that it bordered on being cryptocrystalline.

The euhedral phenocrysts, when identifiable, were mostly sanidine. There were many subhedral phenocrysts of microperthite in the B2t-no.2 pebble. A great many partially resorbed, anhedral phenocrysts of perthite in the IIIC3ca-no.2 pebble were present.

Banding was evident in the B2t-no.1 pebble. There were "stringers" of feldspar (species unidentified) and quartz paralleling the bands. The grain size in these stringers was several times larger than that in the groundmass.

Mafic minerals, both those forming phenocrysts and those in the groundmass, were highly altered. The original minerals could not be identified. The only identifiable alteration products were secondary iron oxides.

In all pebbles, except the IIIC3ca-no.2, the groundmass feldspar

was more extensively altered than the phenocrystic feldspar. In the IIIC3ca-no.2 pebble the difference in the degree of alteration between the groundmass feldspar and that in the phenocrysts was less apparent. However, the extent of alteration differences between the feldspar and quartz in the same pebble was striking. Staining, due to the dissemination of secondary iron oxides, was extensive in three of the slides. Opal filled many of the cavities in the B2t-no.2 section. Some secondary silicate clays were present in the IIIC3ca-no.2 section.

General Discussion of the Musquiz Thin Sections

The thin section studies gave only slight evidence of parent material variability with depth in the profile. The parent material was apparently alluvial outwash debris which was composed of rhyolitic and trachytic rocks of local origin. The feldspar/quartz ratios of the ped thin sections were generally constant, ranging from 1.2 in the B22t horizon section to 3.0 in the strongly impregnated portion of the IIClca horizon slide. The percentage groundmass fragments remained approximately constant with depth through the B22t horizon, substantially increased in the B23t horizon, and then decreased in the IIClca horizon. The decrease in percentage groundmass fragments noted in the IIClca horizon may or may not be significant. The decreased percentage probably reflects the increase in percentage $CaCO_3$ but may indicate that the IIClca horizon has been more extensively weathered than the overlying horizon. If the latter occurred, the material from which the IIClca horizon developed would have been deposited, a soil formed, and then the solum eroded before the material from which the modern overlying

horizons developed was deposited.

The B22t horizon clearly has been the zone of maximum clay illuviation based on cutan percentages. The higher cutan percentage noted in the horizontally cut ped, relative to the vertically cut ped, shows that the clay has been moved downward. The cutans were, in general, not strongly oriented and were classified as ferri-argillans.

Heavy Mineral Studies

In an attempt to determine the relative homogeneity of the parent material from which the Kokernot and Musquiz soils developed, a heavy mineral study was made on the very fine sand fractions of selected horizons. The ratios of light (s.g. <2.95) to heavy (s.g. >2.95) minerals were determined and are given in Table 6. Non-magnetic/magnetic mineral ratios within the heavy mineral fraction are also given in Table 6 as are zircon/sphene ratios. Heavy non-magnetic fractions were embedded and ground to a thickness of 30 microns by the National Petrographic Service Co., Houston. Microscope counts were made to determine percentage composition. The results are shown in Table 7. An average of 600 counts were made on all slides except for that of the Kokernot A1 horizon. There were only about 300 grains present on this slide and the percentages obtained may not be representative. The Musquiz IIIC3ca horizon section was ground so thin that mineral identification was impossible and no percentages were obtained.

Kokernot Soil

Examination of Table 6 shows that the ratios of light/heavy and

non-magnetic/magnetic minerals increase with depth.

TABLE 6

MINERAL RATIOS OF VERY FINE SAND FRACTIONS

Soil	Horizon	Light / Heavy	Non-Magnetic / Magnetic	Zircon / Sphene
Kokernot	A1	36.9	1.7	1.5
	B21t	48.6	2.7	3.7
	R/B22t	48.9	3.6	7.3
Musquiz	A12	20.5	1.1	2.7
	B22t	20.5	1.7	3.1
	IIC1ca	11.5	1.4	3.1
	IIIC3ca	20.8	1.8	

This is attributed to decreased weathering effects at the lower depths and not to changes in parent material. The light minerals, mostly feldspar, and the non-magnetic minerals, containing significant amounts of amphibole, would be more susceptible to weathering than their heavy and magnetic counterparts thus giving lower ratios in the upper horizons. The zircon/sphene ratios are somewhat erratic. Since both zircon and sphene are highly resistant to weathering, the ratios should remain about constant if the parent material was homogeneous. It is believed that the variation between ratios of the horizons is the result of a low number of counts for the A1 horizon section, as was previously noted, and by the difficulty in distinguishing

TABLE 7

NON-MAGNETIC HEAVY MINERAL PERCENTAGES OF

VERY FINE SAND FRACTION

Soil	Horizon	Opaque	Zircon	Sphene	Amphibole	Garnet	Epidote	Pyroxene	Translucent Iron Oxides	Other
Kokernot	A1	49	15	10	1	3				2
	B21t	66	13	4	14	1	1	1	1	1
	R/B22t	67	9	1	17	1	2	1	2	
Musquiz	A12	75	7	3	10	2	2	1	2	<1
	B22t	80	8	2	6	2	1	<1	2	
	IIC1ca	78	9	3	6	1	1	1	1	<1

some sphene particles from zircon. Also, the percentages of minerals which compose the non-magnetic fraction generally show weathering effect differences with depth. An obvious discrepancy is apparent in the percentages noted for sphene. Opaque minerals are dominant and are inherited from the parent rock.

In general, the results indicate that the Kokernot soil developed from a homogeneous parent material. The soil is only moderately weathered as suggested by significant quantities of amphiboles remaining in the A1 horizon.

Musquiz Soil

The light/heavy mineral ratios given in Table 6 show that the A12 and B22t horizons have developed from the same parent material. The significant ratio decrease noted for the IIC1ca horizon is indicative of a lithologic discontinuity. The ratio noted for the IIIC3ca horizon is approximately equal to those ratios noted for the A12 and B22t horizons and shows that the IIIC3ca horizon was apparently formed from a different material than that from which the IIC1ca horizon formed. However, the non-magnetic/magnetic mineral ratio and the zircon/sphene give no indication of parent material variability.

The mineralogical makeup of the heavy non-magnetic fraction shown in Table 7 generally suggests that the parent material is homogeneous at least through the IIC1ca horizon. Individual minerals were present in approximately equal quantities throughout the profile with the exception of amphibole. The higher percentage of amphibole noted in the A12 horizon may indicate surface deposition. Recent surface deposition was also noted in field studies. As in the Kokernot soil, opaque

minerals composed the bulk of the heavy mineral fraction.

In summary, the data indicate that the Kokernot soil has developed from homogeneous material. The Musquiz parent material was apparently homogeneous, at least to the IIClca horizon. The light/heavy mineral ratios of the IIClca and IIIC3ca horizons gave some evidence of a lithologic change in the parent material of these horizons but this evidence was not substantiated by non-magnetic/magnetic ratios, zircon/sphene ratios, or the percentage non-magnetic mineral composition. It is believed that some surface additions of minerals, primarily amphibole, have been made to the Musquiz soil but that the source of these minerals was local.

X-Ray Diffraction Studies of the Silts and Clays

The mineralogy of the Kokernot and Musquiz silt, coarse clay, and fine clay fractions will be discussed in order. The presentation will be made in order of horizon depth in each of the profiles. A detailed discussion of all peaks will be presented for the A horizon patterns of both soils and all comparisons of other patterns will refer to those of the A horizons unless otherwise stated. Figures of the X-ray diffraction patterns are shown with reference peaks labeled. Because of space limitations, only one decimal place of the angstrom (A) spacing numerals are shown on the patterns. However, in determining the d spacings for mineral identification, two decimal places were used. In describing the patterns it was often necessary to use two decimal places to differentiate between peaks. In such instances, an explanation will be given. A glazed porcelain slide was used to mount the coarse and fine clay

samples for X-ray diffraction analysis. Examination of a blank run on the glazed porcelain revealed intense peaks at 4.43A and 3.30A. These peaks are identified in the discussion of the Kokernot R horizon coarse clay patterns since that is the first pattern in the order of horizon discussion in which they are obvious. Identification of the porcelain plate peaks are thereafter omitted.

A concerted effort was made to get equal concentrations of the clay samples on all slides. This was done in an attempt to provide a basis for comparing relative intensities of the peaks. The fact that the glazed porcelain peaks appear on some patterns, but not on others, shows that this effort was not entirely successful. It is believed however, that the consistency with which the 10.0A line increases in intensity upon heating indicates that the increase was, at least, partially caused by collapse of a swelling component.

The small numbers, i.e., 10, 20, 30, etc., which lie parallel to the reference lines are inherent from the original graph paper and could not be removed during reproduction of the X-ray diffractograms. These numbers should be disregarded.

Kokernot Soil

A1 Horizon

Silt-Figure 15. Examination of this pattern reveals three peaks in the immediate vicinity of the 3.2A line. The line labeled 3.2A is actually a 3.21A peak and to its right and left are peaks of 3.24 and 3.19A,respectively. To the right of the lines labeled 3.3 and 2.9A are unlabeled peaks of 3.5 and 3.0A, respectively.

Moving from right to left, the diffraction pattern shows peaks at 4.3, 4.0, 3.8, 3.5, 3.3, 3.24, 3.2, 3.19, 3.0, and 2.9A. The most intense peaks, located at 4.3 and 3.3A are the (100) and (101) reflections, respectively, of quartz. All other peaks are indicative of feldspars. Sanidine is identifiable by reflections at 3.8A (130), 3.24A (202,040), 3.2A (002), 3.0A (131),and 2.9A (222). Plagioclase feldspars are indicated by reflections at 4.0A (201), 3.8A (111), 3.5A (112), 3.2A (040), and 2.9A (220). Identification of individual plagioclase feldspar species is extremely difficult especially in a mixed sample. However, the diffraction peaks shown correspond very closely to andesine and it is believed that this mineral is the dominant plagioclase.

B21t Horizon

Silt-Figure 15. The mineralogy of this fraction was essentially unchanged from that noted for the A1 horizon silt fraction. Almost identical peaks were obtained, the only noticeable difference is an increase in intensity of the 4.0A reflection.

A1 Horizon

Coarse Clay-Figure 15. The pattern obtained from the calcium saturated, glycerol solvated (Ca-glycerated) sample gives no indication of a swelling component in the 17.7A region. A micaceous mineral, identified as illite, is shown by 10.0A (001), 5.0A (002),and 3.3A (003) reflections. The intensity of the 3.3A peak is increased since it coincides with the (101) reflection of quartz. The 7.2A peak is attributed to the (001) reflection of kaolinite. The (002) reflection of kaolinite

appears at 3.6A. Quartz is identifiable by the presence of peaks at 4.3A (100) and 3.3A (101). The weak peaks at 3.2 and 3.0A indicate feldspar.

Analysis of a K saturated sample which had been heated to 250 C (K-250 C) shows a slight increase in the illite (001) and (003) reflections. This is indicative of either one, or both, of two things. Either the 10A peak was increased by collapse of a small quantity of a swelling component, which was not noted by Ca-glyceration, or the concentration of clay on the K-250 C slide was greater than that on the Ca-glycerated slide. In this case, the increased intensity of the illite (001) and (003) reflections is probably due to a combination of the two since the intensity of kaolinite, quartz, and feldspar reflections also is increased. The failure of the illite (002) reflection to increase proportionally to that noted for the (001) reflection cannot be adequately explained.

The pattern obtained by heating the K-250 C sample to 550 C (K-550 C) showed a decrease in intensity of all illite reflections. This decrease in intensity is characteristic throughout all the samples which were analyzed and is believed to be caused by either an alteration in the orientation of the clay or by a partial disruption of the illite structure. Kaolinite is destroyed by heating to 550 C and only illite, quartz, and feldspar reflections remain.

B21t Horizon

Coarse Clay-Figure 15. The mineralogy of this fraction is very similar to that noted in the discussion of the A1 horizon pattern. Overall,

the peaks are sharper and more intense which indicates either more clay on the plate, or a higher degree of crystallinity, or both. The pattern given by the Ca-glycerated sample shows peaks at 10.0, 5.0, and 3.3A which correspond to the (001), (002), and (003) reflections of illite. First and second order kaolinite peaks are shown at 7.2 and 3.6A respectively. Quartz is identifiable by an intense peak at 3.3 and a moderate peak at 4.3A. Feldspars are indicated by weak peaks at 3.2 and 3.0A. There is slight indication of a swelling component that can be detected by examining the pattern in the 17.7A region. No discrete peak is present but there is a broad diffraction band in this region.

The pattern obtained from a K-250 C sample also indicates the presence of a swelling component. The intensity of the 10A reflection is apparently increased by the collapse of the swelling component as indicated by the disappearance of the broad band in the 17.7A region. All of the previously noted orders of illite, kaolinite, and quartz are present in this sample. Feldspars are again indicated by the presence of the peaks noted in the previous discussion. The unmarked peak which lies to the right of the 3.6A line coincides with the 3.8A reflection of feldspar. Heating of the K-250 C sample to 550 C resulted in the disappearance of the kaolinite peak and thus verified its identification.

R Horizon

Coarse Clay-Figure 15. The indicated mineralogy of this clay fraction is not appreciably different from that of the overlying horizons. There is a definite indication of a swelling component as shown by a

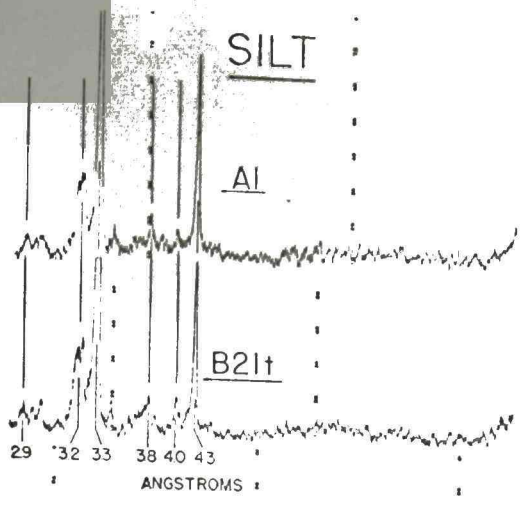

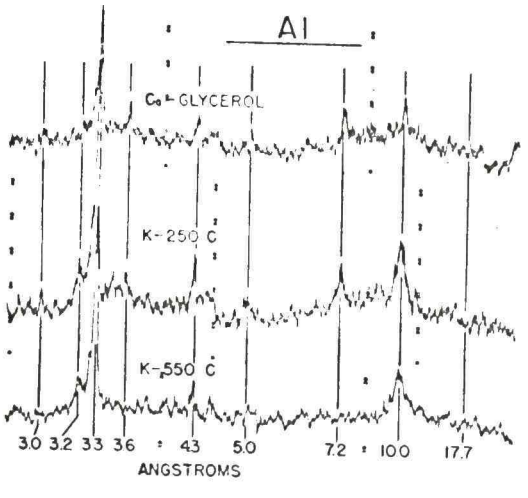

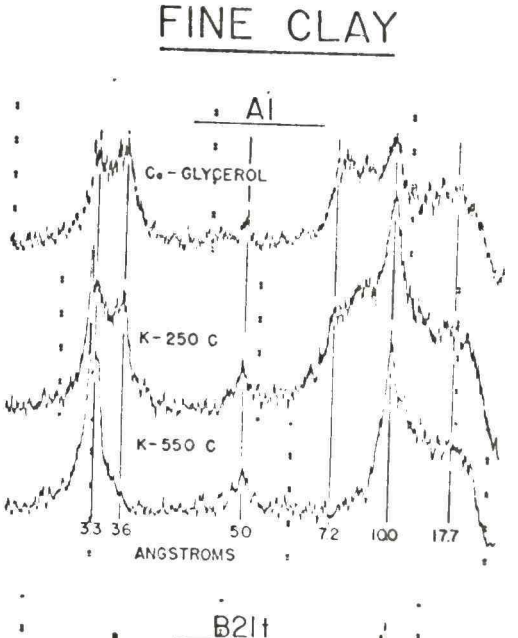

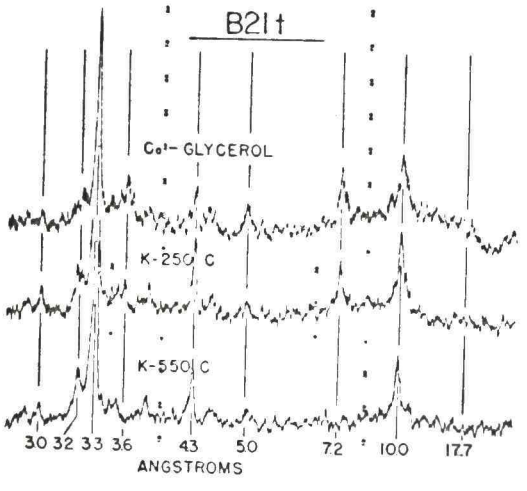

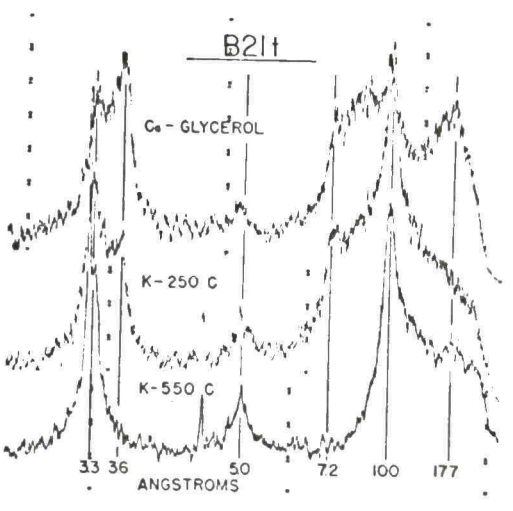

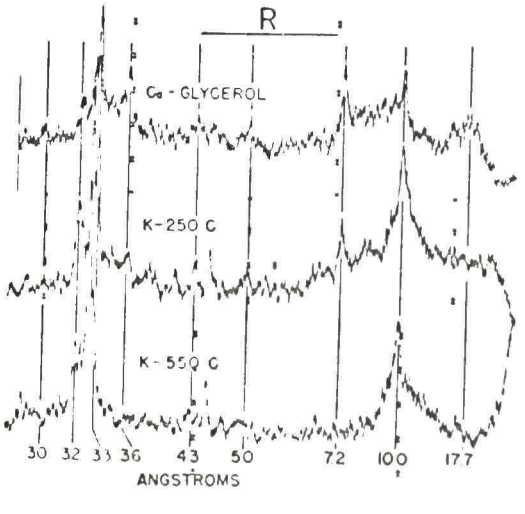

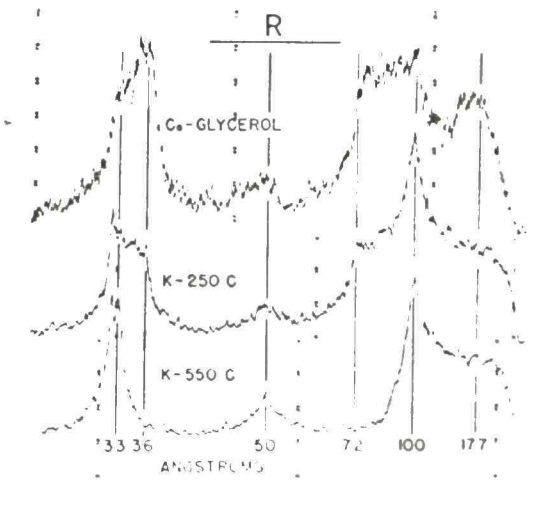

Figure 15. X-ray diffraction patterns of Kokernot silt, coarse clay, and fine clay.

diffuse peak in the 17.7A region of the pattern obtained from the Ca-glycerated sample. Illite, kaolinite, quartz, and feldspar can be identified by the same reflections as were outlined in the discussion of the A1 horizon coarse clay fraction.

The pattern obtained from the K-250 C sample shows an increase in the intensity of the 10A peak which was apparently caused by collapse of the swelling component. Unmarked peaks which lie to the left of the 4.3 and 3.0A lines are 4.0 and 2.9A reflections, respectively, of feldspar. The peaks given by the glazed porcelain slide can clearly be identified on this pattern. They lie to the immediate right and left, respectively, of the lines marked 4.3 and 3.3A.

Heating the slide to 550 C destroyed the kaolinite as is shown by the disappearance of peaks at 7.2 and 3.6A.

A1 Horizon

Fine Clay-Figure 15. The pattern obtained from the Ca-glycerated sample shows a very diffuse peak in the 17.7A region which indicates the presence of a swelling component. Illite is identifiable based on the presence of 10.0A (001), 5.0A (002) and 3.3A (003) reflections. Peaks at 7.2 and 3.6A are attributed to the (001) and (002) reflections of kaolinite. The apparent weak first order illite and kaolinite reflections are attributed to interference by the (002) reflection of the swelling component. This interference can also be noted between the (002) kaolinite and (003) illite reflections.

The pattern obtained from the K-250 C sample shows a definite increase in the 10A peak. This is attributed to the partial collapse of

the swelling component. Failure of the swelling component to completely collapse can be noted by the diffuse reflections in the 17.7A region and by the interference between the first order illite and first order kaolinite peak. This apparent lack of collapse may have been caused by rehydration after heating.

Heating the sample to 550 C resulted in the destruction of kaolinite and a more complete collapse of the swelling component. The swelling component is believed to be a randomly interstratified mixture of illite-montmorillonite. This observation is based on the fact that no discrete peak could be obtained by Ca-glyceration but an increased intensity of the 10A line was obtained by K saturation and heating. No quartz or feldspar was noted in the fine clay fraction.

B21t Horizon

Fine Clay-Figure 15. The pattern obtained by Ca-glyceration of the clay sample definitely indicates the presence of a swelling component in the 17.7A region. The most intense diffraction in this region falls exactly along the 17.7A line and is characteristic of montmorillonite. However, the diffuseness of the peak and the interference noted between illite and kaolinite reflections is indicative of a partially interstratified clay mineral. Illite can be identified by peaks at 10.0, 5.0 and 3.3A. The peaks at 7.2 and 3.6A are characteristic of kaolinite.

The presence of a swelling component can be verified by the pattern obtained from a K-250 C sample. The intensity of all illite reflections were substantially increased by the partial collapse of the swelling

clay type to 10A. Failure of the swelling component to completely collapse can be verified by examination of the area between the first order illite and kaolinite reflections.

The pattern obtained from a K-250C sample shows a continued collapse of the swelling component and complete destruction of kaolinite.

R Horizon

Fine Clay-Figure 15. The pattern obtained from a Ca-glycerated sample from this horizon shows an almost identical mineralogical make-up to that of the overlying B21t horizon. The peaks show a swelling component, illite, and kaolinite at the same spacings and similar intensities as previously outlined.

Saturation of a sample with K and heating to 250 C resulted in a partial collapse of the swelling component and a subsequent increase in the 10A illite peak. Heating of the sample to 550 C destroyed the kaolinite. It should be pointed out that a scale factor of 4, instead of the customary 2, was used on both K saturated samples of this fraction; consequently, the intensity was reduced relative to that which would have been obtained by 100%. The change was necessary to prevent too much of the 10.0 and 3.3A peaks from being off scale.

General Discussion of Silt and Clays

Silt. The mineralogy of the silt fraction appears to remain constant with depth in the profile. Quartz, sanidine, and a plagioclase feldspar, believed to be andesine, were identified. Quartz appeared to be the dominant constituent. However, feldspar reflections are also strong.

Coarse Clay. The coarse clay patterns show that a swelling component, illite, kaolinite, quartz, and feldspars are present. The interstratified component is a minor constituent and is believed to be randomly interstratified montmorillonite-illite in which illite predominates. The component appears to increase with depth in the profile. This conclusion is based on the diffuse peak obtained in the 17.7A region of the Ca-glycerated, R horizon sample. However, this peak may be the result of preferential concentration of the swelling component since the clay obtained from the R horizon was almost entirely illuviated. Amounts of illite and kaolinite do not appear to change appreciably with depth in the profile. This indicates a relatively immature soil in which pedogenic processes have not greatly differentiated horizons. If considerable clay translocation had occurred, illite would have increased with depth more than kaolinite because individual particles of it are usually smaller. The amount of quartz seems to remain about constant with depth whereas feldspar appears to increase slightly. The quartz, being more resistant to weathering, would not be greatly affected whereas the feldspars would tend to decompose more readily under intense weathering in the upper horizons. Precise identification of the feldspars was not possible since many of the peaks were obscure or missing. However, since sanidine and "andesine" were identified in the silt fraction, it is probably that these are the feldspar species that are also present in the coarse clay fraction.

Fine Clay. The mineralogy of this fraction consists of a swelling component, illite, and kaolinite. Inspection of the patterns indicates

that the swelling component, believed to be a randomly interstratified montmorillonite-illite mixture, gives more obvious reflections at about 17.7A with depth in the profile. This could be the result of increased amounts of interstratified clay in the lower horizons caused by preferential movement; by increases in the montmorillonite/illite ratio in the interstratified component; or by a tendency of the interstratified type to alter to discrete montmorillonite; or any combination of the three. The amount of illite and kaolinite are relatively constant throughout the profile. Quartz and feldspars were not identified in the fine clay fraction.

Musquiz Soil

A12 Horizon

Silt-Figure 16. A general examination of the silt patterns obtained from this soil shows that three peaks occur in the vicinity of the line labeled 3.2A, that actually represents a 3.21A d spacing; whereas the peaks to its immediate right and left are 3.23 and 3.19A peaks, respectively. Other peaks that are unmarked but which will be referred to in the discussion of the silts are: the 3.5A peak that lies to the right of the 3.3A line; the peak, 2.9A, which lies to the left of the 3.0A line; and the very weak peak, 3.9A, to the left of the marked 4.0A line.

The pattern of the A12 horizon silt fraction exhibits peaks from right to left of 4.3, 4.0, 3.9, 3.8, 3.5, 3.6, 3.3, 3.23, 3.2, 3.19, 3.0, and 2.9A. The most intense peaks are the (101) and (100) reflections of quartz which are shown at 3.3A and 4.3A, respectively. Sanidine is

identifiable by the presence of reflections at 3.9A (111), 3.8A (130), 3.23A (202,040), 3.2A (002), 3.0A (131), and 2.9A (222). A plagioclase feldspar, believed to be andesine, is indicated by peaks at 4.0A (201), 3.9A ($1\bar{1}1$), 3.8A (111), 3.5A (112), 3.2A (040), and 3.19A (220). The identification of andesine is not conclusive.

B22t Horizon

Silt-Figure 16. The mineralogy of this fraction is very similar to that described for the overlying horizon. Quartz, sanidine, and a plagioclase feldspar are identifiable. The intensity of the reflections characteristic of sanidine is slightly increased whereas those characteristic of plagioclase feldspars are slightly decreased. This is especially noticeable in examining the 4.0, 3.2, and 3.0A reflections. The peaks at 3.23 and 3.19A, which are indicative of sanidine and plagioclase feldspars, respectively, are extremely faint.

IIClca Horizon

Silt-Figure 16. The mineralogy of this fraction is almost identical to that described for the overlying horizon. The intensity of the quartz reflections has decreased slightly. A corresponding, but not necessarily equal, increase in the sanidine peaks can be noted. No change in intensity of the plagioclase feldspar reflections is apparent.

IIIC3ca Horizon

Silt-Figure 16. Quartz, sanidine, and a plagioclase feldspar, believed to be andesine, are identifiable in this fraction. These minerals

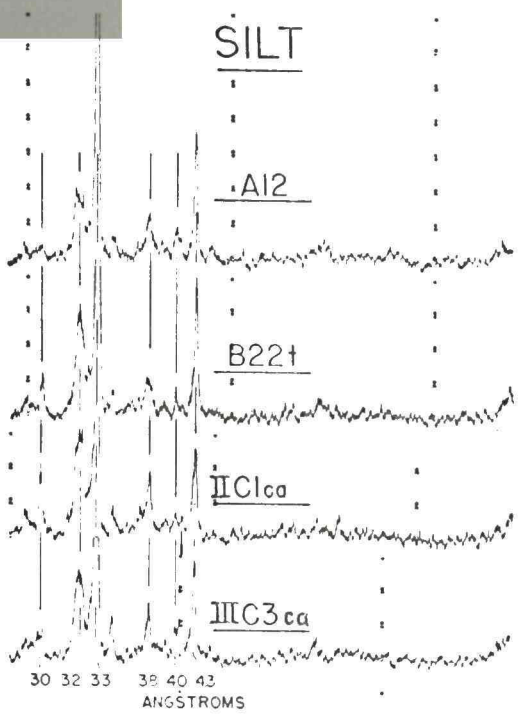

COARSE CLAY

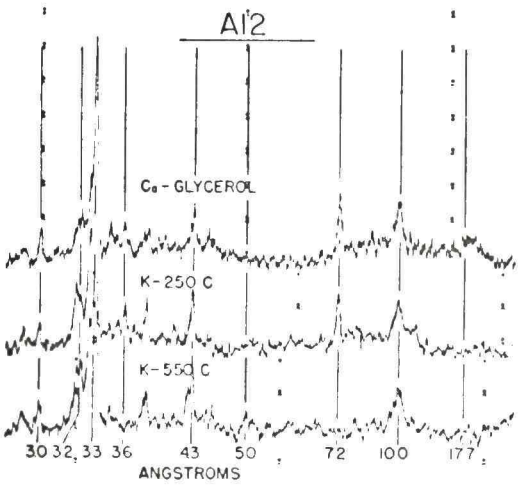

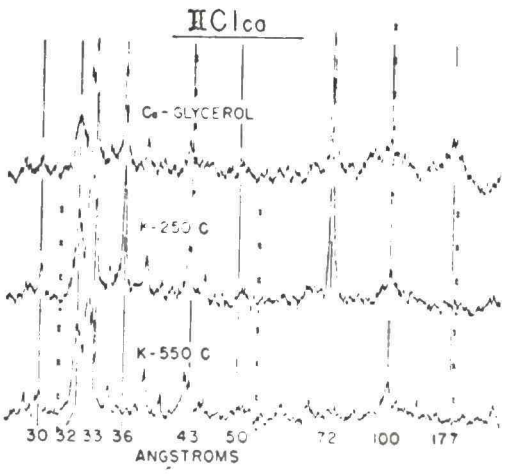

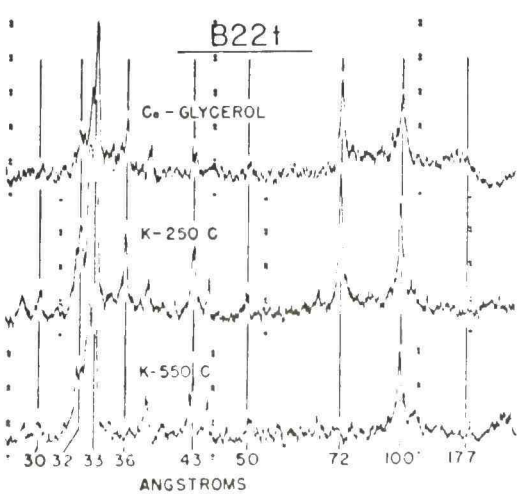

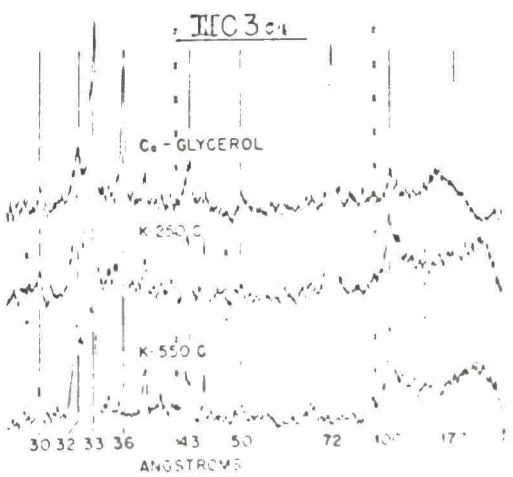

Figure 16. X-ray diffraction patterns of Musquiz silt and coarse clay.

are indicated by reflections identical to those established in the discussion of the A12 horizon sample pattern. In addition to these reflections, there is a strong 4.1A peak which lies immediately to the right of the line marked 4.0A. The 4.1A peak is believed to be the (201) reflection of anorthoclase. The identification of anorthoclase is not conclusive since the most intense reflections from this mineral coincide very closely with those of sanidine and andesine. These reflections are 3.21, 3.24, 3.9, and 3.8A. Other lines are indicative of anorthoclase but their presence on the pattern cannot be established.

A12 Horizon

Coarse Clay-Figure 16. The pattern obtained from a Ca-glycerated sample has lines that are marked from left to right representing 17.7, 10.0, 7.2, 5.0, 4.3, 3.6, 3.3, 3.2, and 3.0A spacings. In addition to the marked reflections, other peaks appear which should be identified. The first of these peaks forms a shoulder upon the larger peak marked 4.3A. This peak represents a 4.2A spacing. One peak appears to the right and another to the left of the line marked 3.6A. These peaks have spacings of 3.8 and 3.5A, respectively. The series of reflections in the vicinity of the 3.2A line are indicative of feldspar, as is the 2.9A peak that lies to the left of the 3.0A line.

A swelling component is indicated by the weak series of reflections in the 17.7A region. Illite is identifiable by the presence of the 10.0A peak. The (002) reflection of illite, at 5.0A, is not present and the (003) reflection, at 3.3A, is masked by the (101) reflection of quartz. First and second order kaolinite lines are present at 7.2 and 3.6A,

respectively. Quartz is identifiable by peaks at 4.3 and 3.3A. Feldspars are indicated by peaks at 4.2, 3.8, 3.5, 3.2, 3.0, and 2.9A.

The trace obtained form the K-250 C sample shows the disappearance of the reflections in the 17.7A region and is believed to be the result of collapse of the swelling component. In addition to those peaks mentioned in the previous discussion, another peak, at 4.0A, lies to the left of the marked 4.3A line and is indicative of feldspar.

The K-550 C pattern shows that kaolinite was destroyed since there are no peaks at 7.2 and 3.6A.

B22t Horizon

Coarse Clay-Figure 16. The pattern obtained from a Ca-glycerated sample of this fraction shows a very similar mineralogical composition to the A12 horizon sample. There is a slight indication of a swelling component in the 17.7A region and illite and kaolinite are identifiable by the presence of their characteristic peaks. Quartz is again indicated, as are feldspars. Characteristic peaks of feldspars at 3.5, 3.0, and 2.9A are only weakly expressed. Assuming equal amounts of clay on each slide of the Ca-glycerated A12 and B22t horizon samples, there appears to be an increase in the amount of kaolinite and possibly illite relative to quartz with depth.

The K-250 C trace shows the disappearance of the reflections in the 17.7A region thus indicating the collapse of the swelling type clay. Feldspar reflections are stronger than in the previously discussed trace.

The K-550 C pattern verifies the destruction of kaolinite.

IIClca Horizon

Coarse Clay-Figure 16. The minerals previously identified in the coarse clay fractions are also present in this sample. The Ca-glycerated sample pattern shows a fairly discrete peak centered around the 17.7A line that is indicative of montmorillonite. The illite reflection is faint and partially obscured by the (002) reflection of the swelling component. Kaolinite, quartz, and feldspars are again identifiable.

The K-250 C trace verifies the presence of a swelling component as shown by the disappearance of the reflection in the 17.7A region. The increased intensity of the 10.0A reflection, relative to that in the Ca-glycerated sample pattern, is believed to be partially caused by collapse of the swelling component and to be partially the result of an increased amount of sample on the slide.

The K-550 C pattern shows that kaolinite was destroyed.

IIIC3ca Horizon

Coarse Clay-Figure 16. The identifiable minerals of this fraction are a swelling component, illite, kaolinite, quartz, and feldspar.

Examination of the trace obtained from the Ca-glycerated sample reveals reflections which lie to the left of the 17.7A region. The reflections are diffuse and no precise spacing can be determined. However, the position of the reflections probably indicates only a partial expansion of the swelling component or that the component is more regularly interstratified than noted in the previously discussed patterns.

The trace from the K-250 C sample reveals a partial collapse of the

swelling component to approximately 10.5A.

Heating of the K-250 C slide at 550 C resulted in a more complete collapse of the swelling component and the destruction of the kaolinite structure.

A12 Horizon

Fine Clay-Figure 17. The trace from the Ca-glycerated sample indicates the presence of a swelling component in the 17.7A region. These reflections are faint and diffuse and no exact spacing can be obtained. The diffuseness of the reflections indicates that the swelling component is not a discrete clay type but an interstratified clay type, probably randomly interstratified montmorillonite-illite. Illite is identifiable based on its (001), (002), and (003) reflections at 10.0, 5.0, and 3.3A, respectively. Kaolinite is indicated by peaks at 7.2 and 3.6A which correspond to the (001) and (002) planes of the mineral.

Verification of the presence of a swelling component can be made by examination of the K-250 C pattern. The intensity of the 10.0A peak is substantially increased by the apparent collapse of the swelling component to 10.0A. Illite and kaolinite are again identifiable.

The K-550 C pattern indicates that kaolinite has been destroyed.

B22t Horizon

Fine Clay-Figure 17. The clay minerals present in this fraction appear to be identical to those described in the A12 horizon. The Ca-glycerated sample pattern shows the presence of a swelling component as can be noted by the diffuse peak in the 17.7A region and in the region

between the (001) reflections of illite and kaolinite. The 17.7A peak is more intense than the peak noted on the A12 horizon sample trace which indicates that the interstratified component has a higher percentage of a swelling type of clay or that it is altering to discrete montmorillonite.

Examination of the K-250 C trace verifies the presence of a swelling component. The partial collapse of the swelling component to a 10A spacing greatly increased the 10.0, 5.0, and 3.3A peaks.

Heating of the K-250 C sample at 550 C resulted in the destruction of kaolinite as is revealed by the absence of the 7.2 and 3.6A reflections.

IIClca Horizon

Fine Clay-Figure 17. The mineralogy of this fraction is somewhat different from that observed for the overlying horizons. The trace from the Ca-glycerated sample indicates the presence of montmorillonite as shown by the strong (001) reflection at 17.7A. The unmarked (002) reflection of montmorillonite, at 8.9A, is represented by the weak peak immediately to the left of the 10.0A line. Illite can be identified by peaks at 10.0, 5.0, and 3.3A. The diffuseness of the 10.0A peak can be attributed to interference by the (002) montmorillonite reflection. Kaolinite is identified by its first and second order reflections at 7.2 and 3.6A.

The pattern obtained from a K-250 C sample shows a definite increase, apparently caused by partial collapse of the montrmoillonite, of the 10.0A peak. The asymmetry of the 10.0A reflection is attributed to the incomplete collapse of montmorillonite. The peak which lies to

FINE CLAY

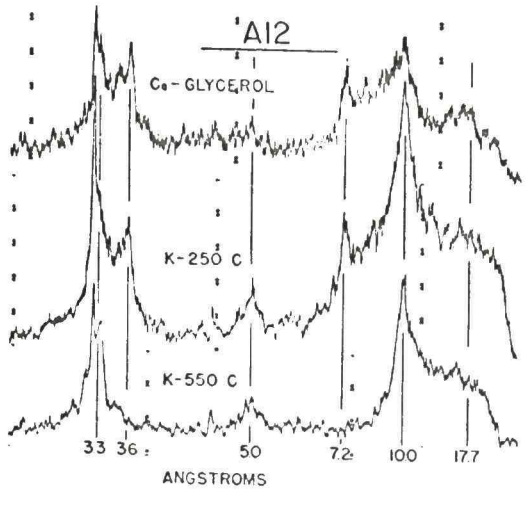

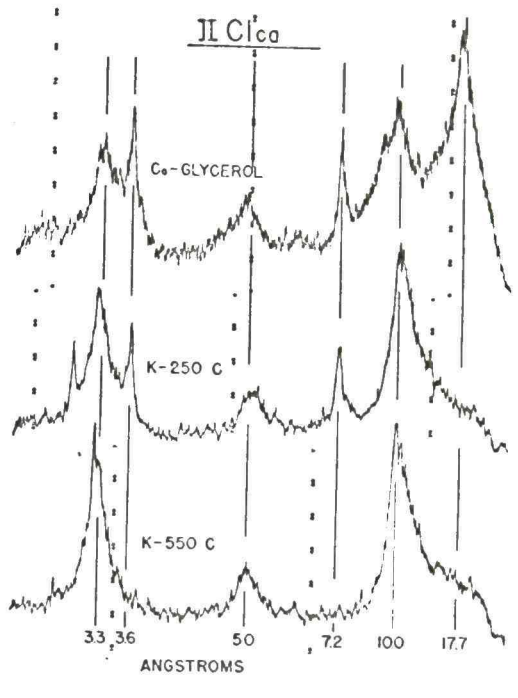

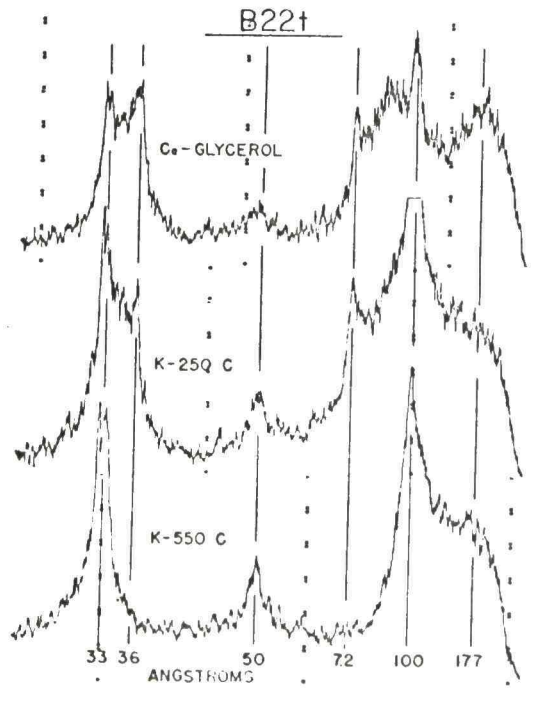

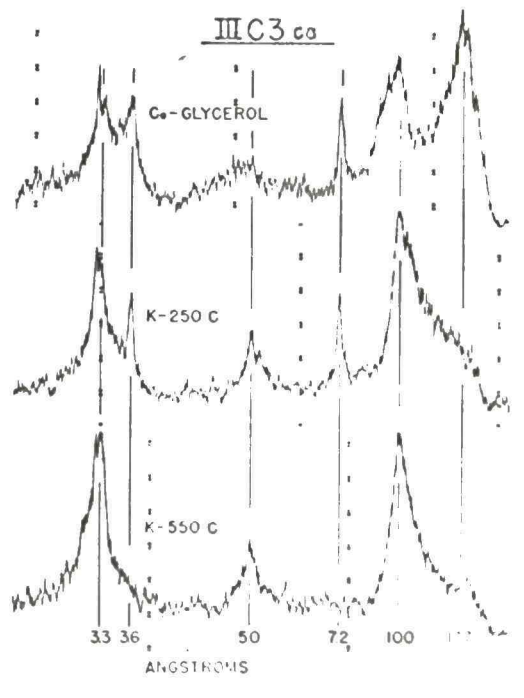

Figure 17. X-ray diffraction patterns of Musquiz fine clay.

the left of the 3.3A line is attributed to KCl which was not completely removed during washing of the sample.

The trace of the K-550 C sample verifies the destruction of kaolinite and the continued collapse of the montmorillonite.

IIIC3ca Horizon

Fine Clay-Figure 17. The mineralogy of this fraction is almost identical to that of the IIClca horizon. The Ca-glycerated trace indicates the presence of montmorillonite, illite, and kaolinite.

Verification of the identification of montmorillonite is obtained by examination of the K-250 C trace. The montmorillonite collapsed and the intensity of the 10.0A peak consequently increased. The diffuseness of the peak is attributed to an incomplete collapse of montmorillonite.

The prior identification of kaolinite was substantiated by the pattern obtained after heating the K-250 C slide to 550 C.

General Discussion of Silt and Clays

Silt. The patterns obtained by X-ray diffraction analysis indicate the presence of quartz, sanidine, and plagioclase feldspars in all horizons. The dominant plagioclase feldspar is believed to be andesine. In addition to these minerals, the IIIC3ca horizon pattern indicates that anorthoclase may be present in substantial quantities. The amount of quartz appears to decrease slightly with depth and an increase in feldspar occurs. This observation is based on the relative intensities of the peaks and may or may not be accurate because of previously stated reasons.

Coarse Clay. The patterns show that a swelling component, illite,

kaolinite, quartz, and feldspars comprise the mineralogy of the coarse clay fraction. The swelling component is believed to be a randomly interstratified montmorillonite-illite clay type. This observation is based on the fact that no discrete peak was obtained by Ca-glyceration but an apparent increase in intensity of the 10.0A peak was obtained by K saturation and heating of the samples. It appears that illite and quartz decrease with depth whereas kaolinite, the interstratified component, and possibly feldspars increase. It is possible that the apparent increase of the interstratified component with depth is the result of incomplete separation of the fine and coarse clay fractions in the lower horizon samples. It has previously been pointed out that problems arose in attempts to disperse samples taken from the IIClca horizon and some fine clay aggregates may be included in the coarse clay fraction. Positive identification of the different feldspar species was not made since certain diagnostic peaks were not clearly shown.

Fine Clay. The mineralogy of this fraction consists of a swelling type component, illite, and kaolinite. The swelling component is believed to be a randomly interstratified montmorillonite-illite mixture that may be altering to a discrete montmorillonite type with depth in the profile. Another possibility is that there is a lithologic discontinuity between the B22t and IIClca horizons. The amounts of illite and kaolinite appear to remain about constant throughout the profile.

Differential Thermal Studies

The results of differential thermal analyses (DTA) of the coarse and fine clay fractions from selected horizons of the Kokernot and

Musquiz soils will be discussed. Since similarities exist between the patterns of all coarse and fine clay samples of each soil, they will be discussed together. The scale of all coarse clay patterns is 20mv/in.; whereas the scale of all fine clay patterns is 50mv/in. This means that the fine clay scale is reduced 2.5 times relative to the coarse clay.

Kokernot Soil

Coarse Clay-Figure 18. The thermograms from this fraction show two endothermic reaction maxima from 110 to 130 C and from 560 to 580 C. The first endotherm can be attributed to the loss of interlayer water from montmorillonite, an interstratified clay type, or possibly illite that contains some interlayer water. Grim (18) has shown that considerable loss of interlayer water from illite often occurs before 100 C; whereas the loss of such water from montmorillonite occurs from 100 to 200 C. He states that in discrete mixtures, such as illite and montmorillonite, the patterns may show the thermal effects of the separate clay minerals with intensities proportional to their relative abundance. With regard to interstratified mixtures, the curves may reflect the individual characteristics of the components or may provide thermal data suggestive of a single mineral.

The endotherm at 560 to 580 C is indicative of the loss of hydroxyl lattice water from kaolinite, illite, and possibly montmorillonite. The temperature at which the loss of hydroxyl water apparently ceases is more indicative of kaolinite.

The weak exotherm which peaks at approximately 60 C is believed to be the result of differences in packing between the clay sample and the inert material. Mackenzie and Mitchell (30) state that lack of uniformity

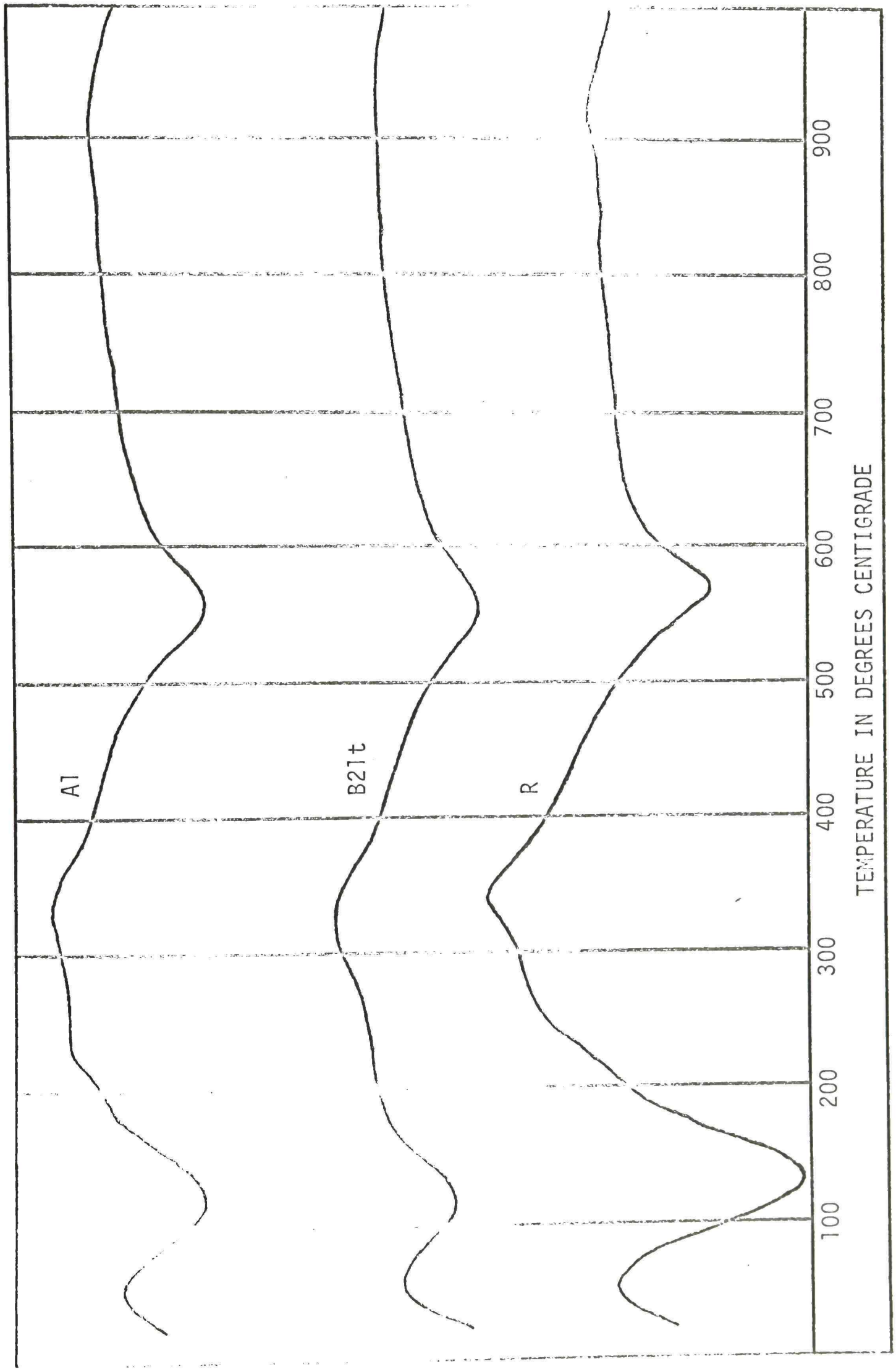

Figure 18. Differential thermograms of coarse clay from the Kokernot soil.

in packing may lead to base line drift, especially at low temperatures. Gruver (19) states that the importance of packing uniformity varies with the kind of material. It is especially important with light, fluffy material but of very little importance for fine grained material. This can be offered in explanation of the fact that the exotherms at 60 C are noted on all coarse clay patterns but are absent on the fine clay patterns. The fine clays when dried formed minute aggregates; however, the coarse clays consisted of individual particles.

The exotherm at approximately 340 C is believed to be the result of oxidation of organic matter. Exotherms at this point only occur in the coarse clay fractions. It is believed that any organic matter which remained after treatment with H_2O_2 would be of such size that it would be removed in the coarse clay fraction during separation of the fine clay from the coarse clay. The increased intensity of the endotherms noted for the R horizon fraction can probably be explained by the nature of the clay. Microscopic studies of the R horizon thin section showed that almost all of the clay was illuviated. It is generally accepted that the smaller clay particles are preferentially translocated. It is believed that the average particle size of the R horizon coarse clay fraction would be smaller than the particles of the overlying horizon coarse clay fractions and an increased intensity of the endotherms would result. The increased intensities could also be caused by incomplete separation of the fine clay from the coarse clay.

Fine Clay-Figure 19. The patterns obtained from this fraction all show two endothermic reaction maxima at 150 to 160 C and 550 to 560 C.

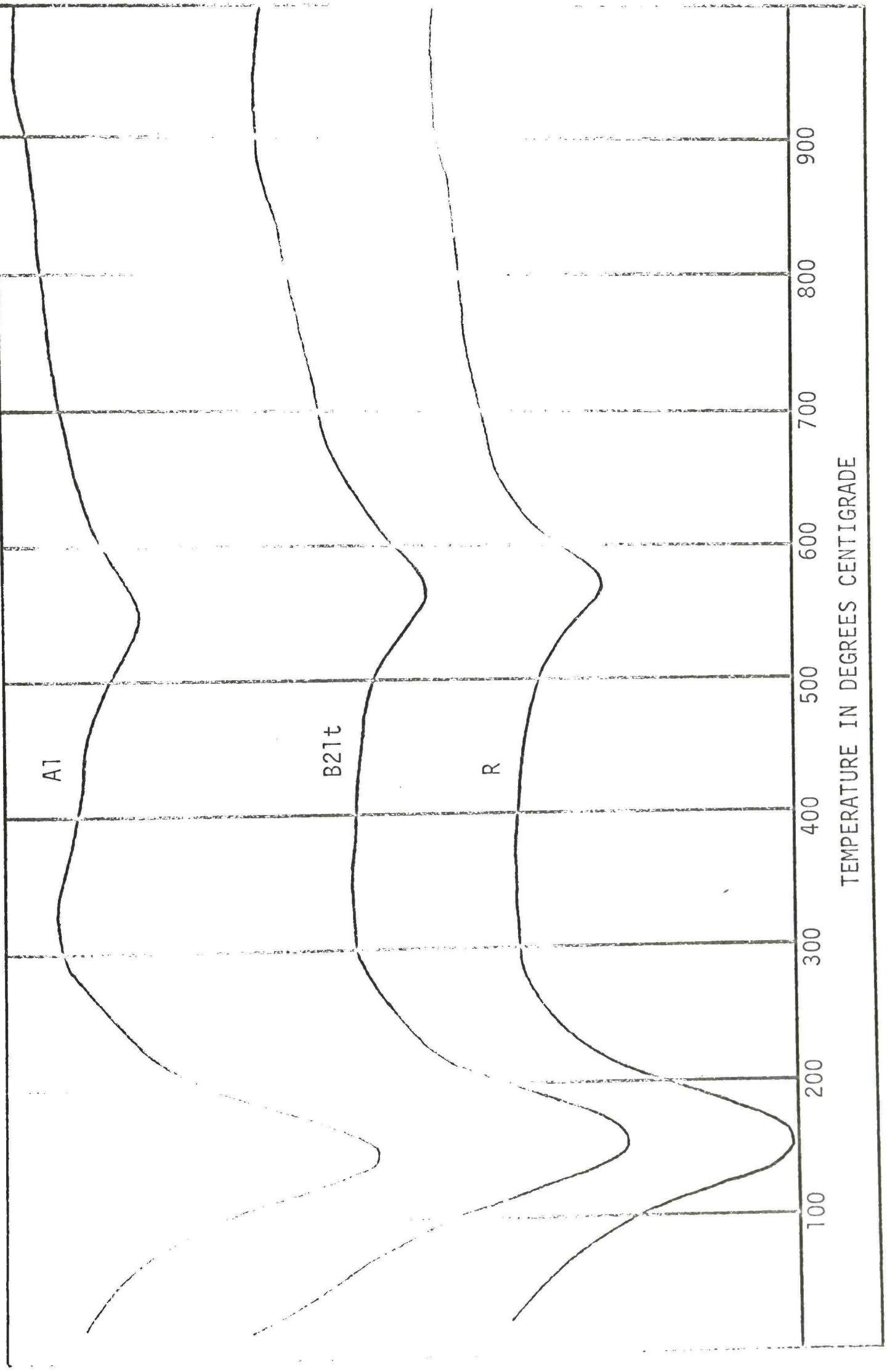

Figure 19. Differential thermograms of fine clay from Kokernot soil.

The strong endotherm at 150 to 160 C is attributed to the loss of interlayer water from montmorillonite or an interstratified clay type. It is possible that some contribution to the endotherm is made by water lost from illite. Another possibility which cannot be discounted is that the endotherm may be partially caused by the presence of amorphous material.

The moderately weak endotherm at 550 to 560 C is believed to be caused by loss of hydroxyl lattice water by kaolinite.

Musquiz Soil

Coarse Clay-Figure 20. The patterns obtained by DTA of these fractions are very similar to those patterns of the coarse clay fractions previously described for the Kokernot soil. The exotherms at approximately 60 C and 340 C are believed to be the result of packing differences between the sample and the inert material and oxidation of organic matter, respectively. All patterns exhibit endothermic reactions from 120 to 125 C and from 570 to 580 C. The endothermic peak from 120 to 125 C is apparently caused by the loss of interlayer water from montmorillonite or an interstratified clay type which contains a swelling component. It is possible that some contribution to the peak intensity was due to interlayer water loss from illite. The endotherm at 570 to 580 C was apparently caused by the loss of lattice hydroxyl water from kaolinite and possibly from some illite.

Fine Clay-Figure 21. The fine clay sample patterns exhibit strong endothermic reactions which peak between 140 and 150 C. The endotherms at this point are believed to be indicative of montmorillonite or an interstratified clay type. It is also possible that the intensity of the

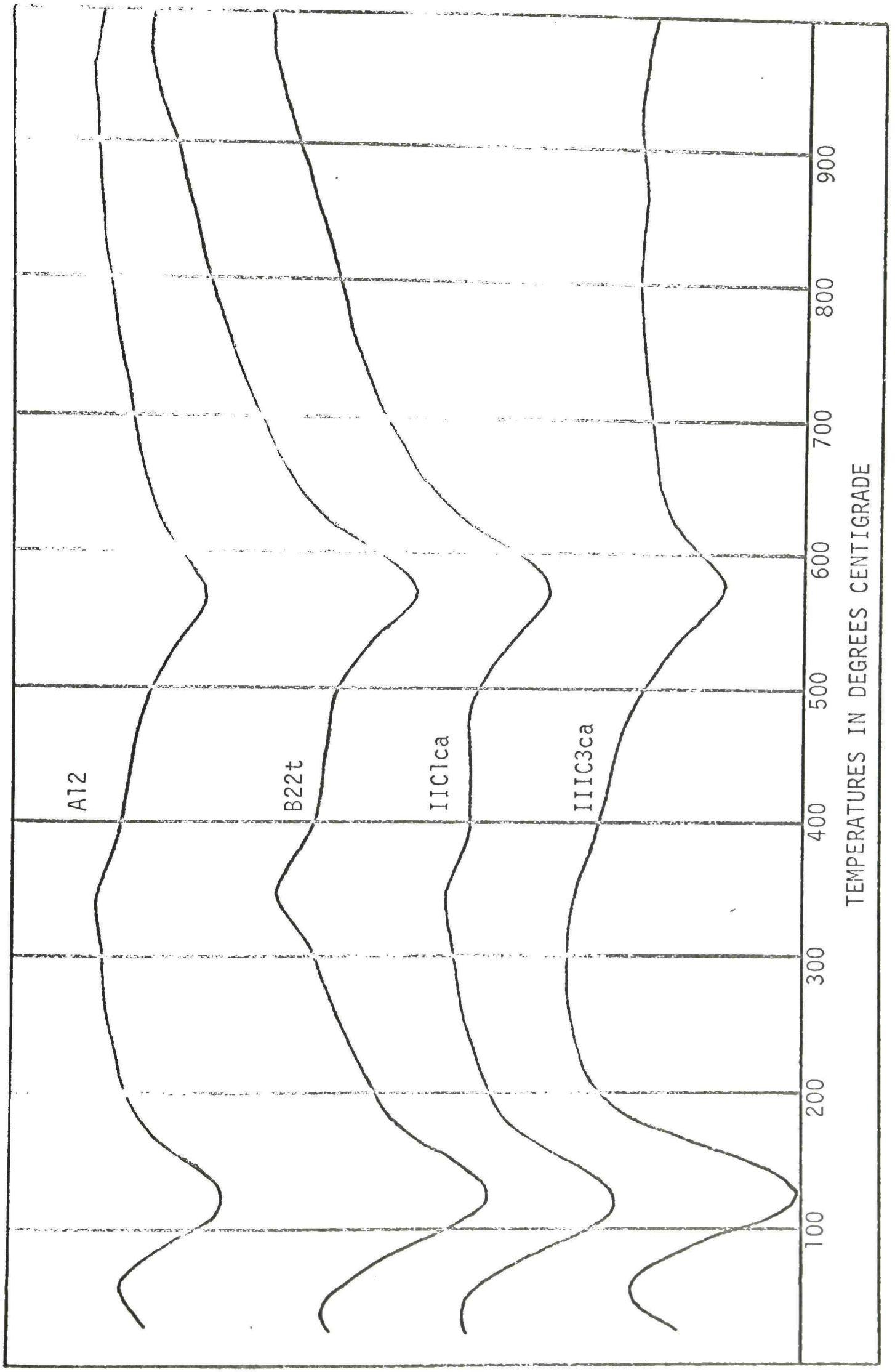

Figure 20. Differential thermograms of coarse clay from Musquiz soil.

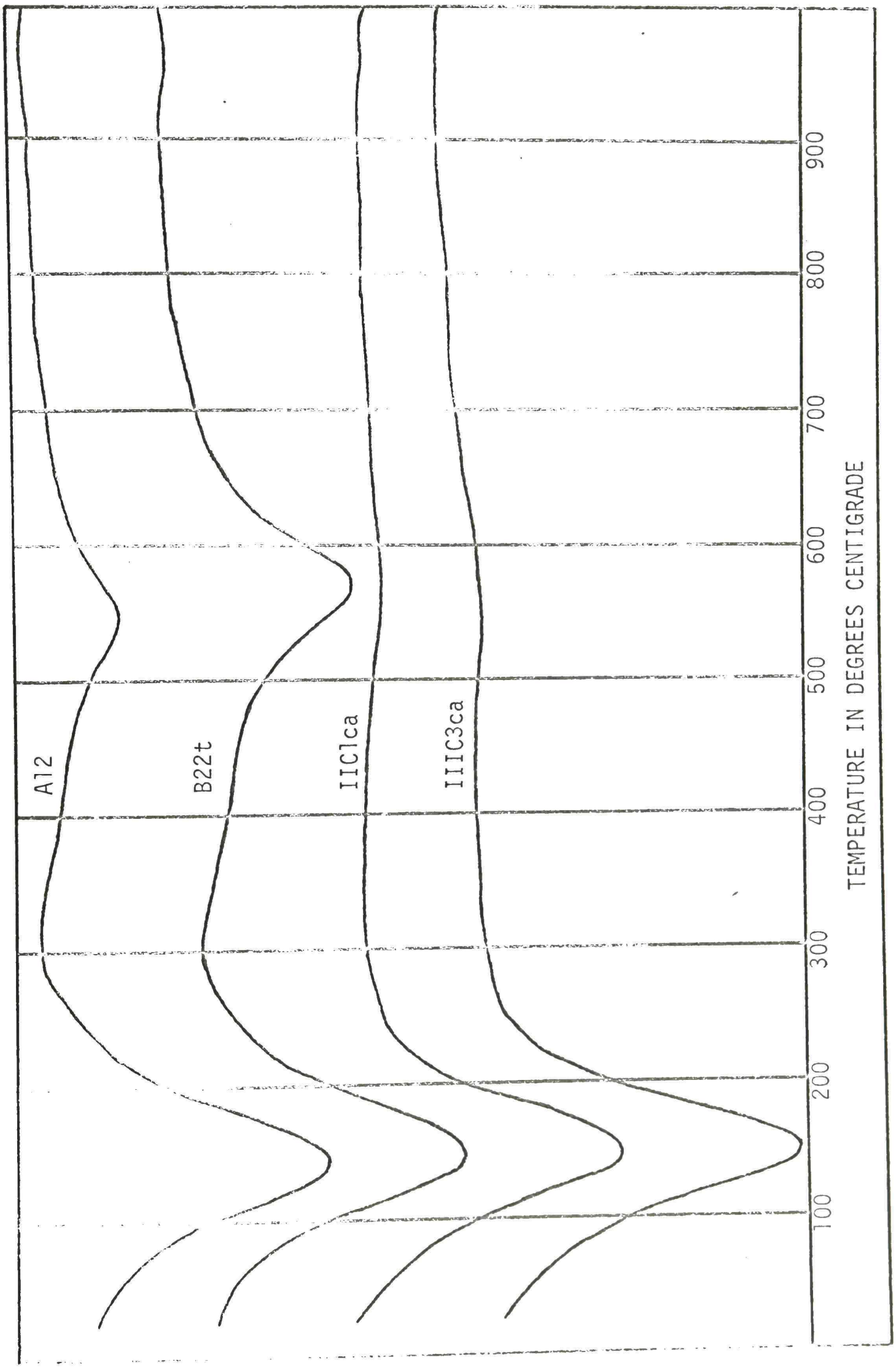

Figure 21. Differential thermograms of fine clay from Musquiz soil.

peaks is somewhat increased by the presence of illite, or amorphous material, or both. The A12 and B22t horizon sample patterns show endothermic reactions which occur at 550 C and 575 C, respectively. These peaks are believed to be primarily the result of lattice hydroxyl water loss from kaolinite. The difference in temperature at which the reaction occurs may be due to differences in the degree of crystallinity of the kaolinite in the samples. It has been shown by Grim (18) that the peak temperature at which thermal reactions occur may be decreased as the degree of crystallinity decreases.

The IIC1ca and IIIC3ca horizon sample patterns show only very faint endotherms at approximately 550 C.

General Discussion of Differential Thermograms

The thermograms of all fractions of both soils indicate the presence of montmorillonite, or an interstratified clay type, or both, and kaolinite. Illite cannot be positively identified. The patterns obtained from the coarse clay fractions of the Kokernot soil show that the proportion of swelling clay increases with depth. Possibly it may be due to incomplete dispersion of >0.2 micron size aggregates that contain some <0.2 micron size particles. The amount of swelling clay apparently remains about constant in the fine clay fraction. The intensities of endotherms indicative of kaolinite increase slightly with depth in both the fine and coarse clay fractions.

The proportion of swelling clay apparently increases with depth in the fine and coarse clay fractions of the Musquiz soil. The amount of kaolinite contained in the coarse clays appears to remain about constant.

The kaolinite endotherm of the fine clay shows an increased intensity in the B22t horizon sample relative to that in the A12 horizon sample. No discrete endothermic peak for kaolinite is discernible in the C horizons.

In general, the DTA results coincide with the results obtained by X-ray analyses. X-ray analyses indicated that kaolinite was present in the fine clay fractions of the Musquiz C horizons. This was not substantiated by DTA. Kaolinite is present but perhaps in such small relative proportions as to not be detected by DTA.

Cation Exchange Capacity Studies of the Silts and Clays

The CEC values of the silt, coarse clay, and fine clay fractions of selected horizons from each soil are given in Table 8. The values are averages of duplicates for all samples.

Kokernot Soil

Silt. The CEC values of this fraction decrease with depth in the profile but overall are higher than would be expected. The high values are probably partially caused by the inclusion of silt size clay aggregates in the samples or by the presence of incipient clay which may have formed in crevices and along cleavage planes of the feldspars. The high feldspar content of the silt fraction also would contribute to the CEC. Marshall (32) states that the exact CEC of feldspar surfaces is exceedingly variable, being dependent on the nature of the saturating ion as well as the ion being released. The possibility of amorphous material, contained in aggregates, contributing to the CEC of the silt fraction

should also be considered.

Coarse Clay. The CEC's of two samples selected from the A1 and B21t horizons were determined. The CEC's are considered to be high for the coarse clay fraction. The values show that the mineralogy of the samples could be almost entirely illite or a mixture of a swelling type clay, illite, and kaolinite. X-ray diffraction analyses, and to some extent DTA, indicated that a swelling component, illite, kaolinite, feldspar, and quartz were present. Since the percentage potassium oxide (K_2O) of the fraction, to be discussed later, indicated that illite could compose only 20% of the coarse clays, the high CEC values obtained indicate that a swelling component is present in significant quantities.

Fine Clay. The CEC values of the samples increase with depth in the profile. The values indicate that a high amount, either as discrete particles, or as a constituent of the interstratified component, of the fine clay fraction is composed of a swelling type clay. The proportion of swelling clay apparently increases slightly relative to other clay types with depth. Of course, the increased external surface, of the finer particles would increase the CEC an undetermined amount.

Musquiz Soil

Silt. The CEC values of the silt fractions from each horizon of this soil decrease slightly with depth through the B23t horizon and then increase with depth throughout the C horizons. The overall values are higher than expected. The high values are apparently partially caused by silt size clay aggregates being included in the silt fraction

although the presence of silicate layer clays was not noted in X-ray studies. It is also possible that incipient clay formation in the feldspar grains contributes to the CEC's of this fraction. The extremely high value of the IIIC4 horizon sample could only be caused by the presence of silicate clay minerals, or amorphous material, in significant quantities. This value reflects the poor dispersion and separation obtained for this sample.

Coarse Clay. The CEC values of selected horizon samples show a decrease with depth through the IIClca horizon. The value for the IIIC3ca horizon sample is significantly higher than that of the overlying IIClca horizon sample. The values indicate that the mineralogy of this fraction is mixed, probably composed of illite, kaolinite, and an expanding clay. The extremely high value of the IIIC3ca horizon sample could only be caused by the presence of an expanding component, or amorphous material, or both. Again, this probably reflects poor dispersion. X-ray diffraction analyses, and to a lesser degree DTA, confirmed the presence of a swelling component, kaolinite, and illite. The presence of amorphous material in the IIIC3ca horizon sample was indicated by the tendency of this sample to peel from the glazed porcelain slide when samples were being prepared for X-ray analysis. As has been previously stated, removal of amorphous material decreased the tendency of the samples to peel.

Fine Clay. The CEC values of this fraction increase slightly with depth through the IIClca horizon and then decrease. The high values noted for all horizon samples indicate a high proportion, probably in excess

of 50%, of a swelling type clay in this fraction. Assuming that an expanding component composes approximately 50% of the fine clay fraction, the second most important clay type would be illite. Kaolinite would be a minor constituent. Apparently, the proportion of a swelling type clay increases slightly with depth through the IIClca horizon and then decreases.

Total Potassium Content of the Silts and Clays

The percentage K_2O was determined for the silt, coarse clay, and fine clay fractions of selected horizons. The results, averages of duplicates, are given in Table 8. All fractions from each soil will be discussed together. The K_2O content of the fractions is believed to be derived primarily from interstratified species, illite, or feldspar depending on the fraction in question. Bradley and Grim (9) found that the percentage K_2O of three illites ranged from 6.09% to 6.93%. Jackson and Mackenzie (24), in discussing the chemical analysis of illites, states that a percentage K_2O of 6.5 is the mean number of published analyses and is representative of hydrous micas in which some potassium has been replaced by other cations. These authors stated that in micas of full K content, the figure of 10% K_2O is often used. Calculations for feldspar reveal that the pure K end member ($KAlSi_3O_8$) contains approximately 16 to 17% K_2O. The percentage K_2O of the feldspar would decrease with increasing amounts of Ca and Na replacing the K. X-ray and microscopic analyses of the fractions indicated that sanidine was the dominant feldspar. Assuming equal amounts of Na and K and an arbitrary formula of $(NaK)AlSi_3O_8$ for sanidine, the K_2O content would be

TABLE 8

SELECTED CHEMICAL DATA OF THE SILTS AND CLAYS

Soil	Horizon	C.E.C. Meq./100 gms.			Percentage K_2O			Percentage SiO_2		Percentage Al_2O_3	
		silt	0.2-2.0μ	<0.2μ	silt	0.2-2.0μ	<0.2μ	0.2-2.0μ	<0.2μ	0.2-2.0μ	<0.2μ
Kokernot	A1	11.9	36.1	59.2	0.82	0.94	0.55		6.1		6.9
	B1	11.1									
	B21t	10.0	29.4	64.4	0.88	1.12	0.54		5.3		6.4
	R/B22t	10.0									
	R										
Musquiz	A12	12.5	34.2	67.4	0.95	1.18	0.64		7.1		7.2
	B21t	9.9									
	B22t	9.3	32.0	68.8	1.21	1.36	0.60		5.0		6.2
	B23t	9.7									
	IIC1ca	11.5	29.3	76.3	1.45	1.56	0.58	2.31	5.0	1.38	2.9
	IIC2	13.0									
	IIIC3ca	13.4	47.6	69.4	1.26	1.34	0.56	4.24	5.8	2.01	2.8
	IIC4	25.4									

approximately 8 to 9%. Usually the Na/K ratio is greater than one.

Kokernot Soil

The K_2O content of the silts was attributed almost entirely to potassium feldspars. The percentages show a slight increase with depth in the profile. This increase is probably caused by decreased weathering effects at lower depths. The figures indicate that potassium feldspars compose from 10 to 15% of the silt fractions.

The K_2O content of the coarse clay fractions was believed to be due to both illite and potassium feldspar. The relative proportion of each component cannot be estimated with accuracy. However, assuming an average of 6.5% K_2O for illite, the maximum amount of illite which could be present in the coarse clay fraction would be less than 20%.

The K_2O content of the fine clays was attributed primarily to illite. There is a slight decrease in percentage with depth but it is not considered significant. The percentage K_2O indicates that illite composes slightly less than 10% of the fine clay fraction.

It is realized that the variability which may occur in K_2O content of illite and feldspars reduces the reliability of estimating their percentage in the fractions. However, this data will be used to supplement other analytical data. Since X-ray diffraction analyses indicated an interstratified clay type, believed to be montmorillonite-illite, it is quite possible that the illite has lost significant quantities of potassium.

Musquiz Soil

The K_2O content of the silt fractions shows an increase with depth through the first three horizons. This indicates a slightly higher proportion of potassium feldspar with depth in the silt fraction and is probably due to decreased weathering effects. The K_2O percentage of the IIIC3ca horizon silt fraction decreases relative to the IIClca horizon fraction. The decrease is possibly caused by the inclusion of clay particles in the silt fraction as has been previously noted. Another possibility is that it reflects a lithologic discontinuity in the profile. Assuming an average K_2O content of 8% for the feldspars, the feldspar content of the silt fractions would range from 10 to 15%.

The K_2O percentages for the coarse clay fractions follow essentially the same trend as described for the silt fractions but are slightly higher. The K_2O content of the coarse clays is believed to be due to both potassium feldspars and illite. If the total K_2O contend of the coarse clays were attributed to illite, this mineral could compose from 15 to 23% of the fractions. The lower K_2O content of the IIIC3ca fraction is attributed to the probable inclusion of fine clay aggregates. Neither can a lithologic discontinuity be discounted.

The fine clay K_2O content can be attributed almost entirely to illite. A slight decrease in K_2O percentages with depth occurs but is considered to be insignificant. Apparently, illite composes less than 10% of the fine clay fractions.

Free Silica and Alumina Studies

Rapid dissolution tests for determination of the amount of free silica, alumina, and amorphous aluminosilicates were made on selected clay fractions of the Kokernot and Musquiz soils. The results expressed as percentages SiO_2 and Al_2O_3 are given in Table 8. It is generally accepted that amorphous materials are of small particle size and therefore would concentrate in the fine clay fraction. However, various properties, observed in the laboratory, indicated that the coarse clays of the Musquiz IIClca and IIIC3ca horizons might contain amorphous materials and these samples were included in the tests.

The results are somewhat erratic, both in percentage SiO_2 and Al_2O_3 as well as in the SiO_2/Al_2O_3 ratios. No trends with depth in the profile can be established. The results are extremely difficult to evaluate simce total SiO_2 and Al_2O_3 were not determined. However, comparison of the results in Table 8 with those results obtained by Hashimoto and Jackson (20) indicate that amorphous materials are present in significant quantities. For example, these investigators stated that a kaolinitic clay which contained appreciable quantities of amorphous material released 6.98% SiO_2 and 4.14% Al_2O_3 when subjected to the differential dissolution treatment. Montmorillonitic clays, stated to contain large amounts of allophane-like materials, released a maximum of 12.2% SiO_2 and 4.92% Al_2O_3 when subjected to the same treatment. It is possible that the percentages of SiO_2 and Al_2O_3 shown in Table 8 are significantly increased by the presence of poorly crystallized clay minerals, particularly the interstratified types. Hashimoto and Jackson have shown that as the degree of crystallinity decreases,

increased quantities of SiO_2 and Al_2O_3 are dissolved during the differential dissolution treatment.

CHAPTER VI

SUMMARY AND CONCLUSIONS

Homogeneity of Parent Material

Combined results show that the parent material of the Kokernot soil is homogeneous throughout. The minerals identified by X-ray and microscopic analyses in the >2 micron fractions were mostly released by physical weathering of the parent rock.

Microscopic studies of the Musquiz soil revealed some evidence of parent material variability with depth. The minerals identified in each horizon were qualitatively very similar throughout the profile and their percentages, in general, reflected only normal weathering trends with depth. However, the size distribution of the sand fractions and, to a lesser extent, the mineral ratios within the very fine sand fractions indicated a lithologic change in the parent materials between the B22t and the IIC1ca horizons. Another lithologic change was shown between the IIC1ca and IIIC3ca horizons. It is realized that the lithologic discontinuities may occur within the B23t and IIC2 horizons, respectively, but since detailed analyses were not made for these horizons, the changes were placed at the B23t - IIC1ca and the IIC2 - IIIC3ca horizon boundaries. The variability in parent material was also reflected in the clay mineralogy of the Musquiz soil. The similarities of the minerals identified in both the Kokernot and Musquiz soils are striking; but quantitative differences indicate that the Musquiz soil is more extensively weathered. Apparently, the source

of the alluvial debris from which the Musquiz soil developed came from local sources and has been only slightly contaminated by recent aeolian material.

Clay Mineralogy

Kokernot Soil

X-ray, DTA, K_2O, and CEC results indicate that the coarse clay fractions are composed of quartz, feldspars, kaolinite, illite, and an interstratified montmorillonite-illite. The fine clay fractions contain the same minerals with the exception of quartz and feldspars. The amount of interstratified clay, or montmorillonite, or both, increases slightly relative to illite with depth in both fractions. This increase is believed to be the result of preferential translocation of the smaller size interstratified clay particles and not to differential formation with depth. Estimates of the relative proportion of the clay mineral species are shown in Table 9.

The mode of clay formation is extremely difficult to visualize. Apparently, decomposition of feldspars, with a concurrent loss of K and Na, and a subsequent reconstitution of a layer silicate, resulted in the initial formation of illite. The illite, once formed, was subjected to weathering, lost significant quantities of K from the interlayer positions, and was altered to the interstratified clay type. This mode of formation was indicated by K_2O analysis. The K content of the clays was lower than expected considering that K-feldspars were present in significant amounts in the coarse clays as determined by X-ray analysis. It is possible that a montmorillonite-

like mineral was initially formed instead of illite. The "montmorillonite", by incorporation of K in the interlayers, could have been transformed into illite or an interstratified clay type. However, the preponderance of K bearing minerals relative to Mg bearing minerals would likely favor the initial formation of illite.

TABLE 9

ESTIMATED RELATIVE PROPORTIONS OF CLAY MINERAL SPECIES

Soil	Horizon	Clay Mineral			
		Interstratified Clay	Montmorillonite	Illite	Kaolinite
Kokernot	A1	XXXX	X	XX	X
	B21t	XXX	XX	XX	X
	R	XXX	XX	XX	X
Musquiz	A12	XXXX	X	XX	X
	B22t	XXX	XX	XX	XX
	IIC1ca	X	XXXX	XX	X
	IIIC3ca	X	XXXX	XX	X

Predominant - XXXX; Frequent - XXX; Common - XX; Trace - X.

A question may be raised concerning the occurrence of montmorillonite and illite, mostly interstratified, along with kaolinite in a clay mineral assemblage. Of course, one of the species may be in a metastable condition but assuming that such is not the case, can they occur in equilibrium? Hess (22) has attempted to establish equilibrium

conditions for several mineral pairs in the K_2O-Na_2O-Al_2O_3-SiO_2-H_2O system at 25 C and one atmosphere. He tentatively placed the illite-kaolinite equilibrium at log K^+/H^+=5.5 and -log SiO_2=3.2. He placed the illite-montmorillonite assemblage in an area between log Na^+/H^+=5.4 and log Na^+/H^+=9. The kaolinite-Na montmorillonite values obtained by extrapolation of hydrothermal data were Na^+/H^+=5.9 to 9. The -log SiO_2 boundary ranged from 3.3 to approximately 3.9 varying with log Na^+/H^+ values.

Before the question raised above can be answered, ion activities of Na, K, and H would have to be determined. Potassium activity should be considerable judging from the high K-feldspar content. However, H activity, considering pH measurements, was unexpectedly high. If the log K^+/H^+ value is sufficiently low the illite in the soil may be altering to either kaolinite or montmorillonite depending on log Na^+/H^+ and -log SiO_2 values. Alteration of montmorillonite to kaolinite would depend upon -log SiO_2 values. No projections can be made at present concerning either Na or SiO_2 activities.

Musquiz Soil

Combined results of the studies indicate that the coarse clay fractions are composed of quartz, feldspars, illite, kaolinite, and an interstratified montmorillonite-illite. The fine clay consists of kaolinite, illite, and an interstratified montmorillonite-illite in the horizons which overlie the IIClca horizon. The fine clay from the IIClca and IIIC3ca horizons consists of kaolinite, illite, and montmorillonite. X-ray, K_2O, and differential thermal analyses show that

the proportion of illite and kaolinite decreases slightly with depth while the interstratified clay type, montmorillonite, or both, proportion increases. Electron micrographs of the B22t horizon fine clay fraction, made by Mr. John L. Brown, Consulting Physicist, 1676, Moore's Mill Rd., Atlanta, Georgia, revealed that the clay particles are plate-like and are often frayed around the edges. No fibrous or tubular shaped particles were observed. Table 9 shows estimates of the relative proportion of the clay mineral species.

The mode of clay formation in this soil is believed to be similar to that described for the Kokernot soil in the upper horizons. The abrupt transition from the interstratified montmorillonite-illite in the B22t horizon to discrete montmorillonite in the C horizons partially reflects the lithologic change in parent material. The accumulation of Ca and Mg in the IIClca and IIIC3ca horizons should favor the formation of montmorillonite. The presence of kaolinite in such an environment is difficult to explain. However, DTA indicates that this mineral is present in the C horizons in relatively small quantities.

Approximately the same generalizations that were made concerning the clay mineral assemblage of the Kokernot soil can be made for the clay assemblage of the Musquiz soil. It should be pointed out, however, that the Musquiz soil is not subject to free leaching and the H activity in the lower horizons should be considerably lower than that occurring in any of the Kokernot soil horizons. The Ca and Mg activities in these horizons should be increased because they are zones of carbonate accumulation as stated previously. The possibility of kaolinite being residual in these horizons cannot be completely discounted.

Pedogenesis

Kokernot Soil

Evidence of both physical and chemical weathering in this soil is present. Physical weathering was probably most important in the early stages of soil formation and brought about the initial fracturing of the bedrock. Physical weathering effects at present are believed to be minor although temperature fluctuations probably induce the disintegration of the larger rock fragments. Physical weathering, by reducing the size of fragments, has increased the chemical weathering rate by increasing the surface area of the fragments. Field observations indicate that water percolation through the profile is rapid. This would tend to increase the chemical weathering rate by removing the soluble products of weathering. The rate of water movement through the profile is increased by the presence of significant quantities of gravel.

An obvious direct effect of chemical weathering, as revealed in the microscopic studies, is the alteration of unidentified dark minerals in the parent rock. Of course, the clay in the soil is an indirect result of chemical weathering, i.e., the decomposition of primary minerals and subsequent recrystallization as silicate clays.

Clay translocation has occurred to a limited extent throughout the profile. Microscopic studies revealed, however, that clay movement is not as prevalent as indicated by particle size distribution analyses. Additions of organic matter to the soil surface and its subsequent distribution throughout the profile have been instrumental in ped formation and coloring of the soil. To a limited degree, aggregation has probably

been enhanced by the presence of small quantities of amorphous materials. The aggregation of soil particles would in turn encourage soil structure development.

The profile is considered to be relatively immature since weatherable minerals, principally feldspars and amphiboles, are present in the upper horizons. The presence of quartz in the coarse clay fraction partially reflects the effects of physical weathering and partially the microcrystalline texture of the trachyte groundmass.

Musquiz Soil

In general, the pedogenic processes which were instrumental in forming the Kokernot soil are also involved in the formation of the Musquiz soil. The major differences which exist between the two soils primarily reflect the degree to which the pedogenic processes have occurred.

The Musquiz soil is considered to be moderately weathered and relatively mature. The nature of the parent material (valley fill debris) certainly suggests that significant physical breakdown had occurred before soil formation began and undoubtedly is still occurring, at least, in the upper horizons. Particle size reduction by physical weathering would automatically bring about increased chemical weathering due to increased surface area.

Significant clay translocation has occurred as is evidenced by the increase in clay percentage with depth, fine clay/coarse clay ratios, and the presence of thick cutans as revealed by microscopic studies. Free iron oxides, released during chemical weathering of dark minerals, has also been translocated to a lesser degree. These iron

oxides are often clay size and have affected the soil color in the middle horizons. Organic matter additions have undoubtedly influenced soil color and structure formation in the upper horizons. Significantly, but to a lesser degree than in the Kokernot soil, the presence of gravel has increased water movement through the soil and enhanced horizon differentiation.

Proposed Classification of the Soils

It has previously been stated that the Kokernot and Musquiz are tentative series names for the soils in this study. These soils were classified on the basis of information obtained in the study and using the classification criteria outlined in the 7th Approximation (37). Certain soil properties used as classification criteria in the 7th Approximation were not determined and it was necessary to make some assumptions. However, near the end of the study, difficulty was encountered in classification of the soils into subgroups. Additional information was needed on exchangeable K with depth in the profiles. Exchangeable K determinations were made on selected horizons of each soil using the method outlined in U.S.D.A. Handbook No. 60 (42) Exchangeable K decreased from 1.0 meq./100 gm. in the A1 horizon of the Kokernot soil to 0.8 meq./100 gm. in the B21t horizon. Exchangeable K in the Musquiz soil increased from 0.9 to 1.7 meq./100 gm. in the A12 and B22t horizons, respectively. It was assumed that the distribution of exchangeable Na would be similar to the distribution of exchangeable K.

The soils were tentatively classified as follows:

Kokernot Soil	
Order	Alfisol
Suborder	Ustalf
Great Group	Haplustalf
Subgroup	Lithic Udic Haplustalf*
Family	Fine loamy, mixed, thermic
Musquiz Soil	
Order	Mollisol
Suborder	Ustoll
Great Group	Argiustoll
Subgroup	Typic Argiustoll
Family	Fine, mixed, thermic

Suggestions for Further Study

Further studies of the clay fractions of both soils, especially the interstratified clay, are needed. The establishment of parameters for the formation of the interstratified species would be especially worthwhile.

Determination of the percentage amorphous material and its precise effect on the physical and chemical properties of the soils would be helpful.

The low pH's of the soils was surprising. Percentage base saturation determinations would perhaps shed light on this subject.

---

*"Lithic Udic Haplustalfs" are a proposed subgroup. The subgroup would be like the established "Udic Haplustalfs" except that they would have a lithic contact within 20 inches of the surface.

LIST OF REFERENCES

1. Albritton, C. C., Jr., and Bryan, K. Quaternary Stratigraphy in the Davis Mountains, Trans-Pecos, Texas. Geol. Soc. Amer. Bull. 50:1423-1474, 1939.

2. Allen, B. L. A Mineralogical Study of Soils Developed on Tertiary and Recent Lava Flows in Northeastern New Mexico. Thesis for the degree of Ph.D., Michigan State Univ. pp. 76-78, 1959.

3. Aomine, S. and Yoshinaga, N. Clay Minerals of Some Well-drained Volcanic Ash Soils in Japan. Soil Sci. 79:349-356, 1955.

4. Baker, C. L. and Bowman, W. F. Geologic Exploration of the Southeastern Front Range of Trans-Pecos, Texas. Univ. of Texas Pub. 1753: Publ. by Bureau of Economic Geology, Univ. of Texas, 1917.

5. Baver, L. D. Soil Physics. Third Edition. John Wiley and Sons, Inc., New York, pp. 55-63, 1963.

6. Birrel, K. S. Surface Acidity of Subsoils Derived from Volcanic Ash Deposits. New Zeal. J. Sci. 5:453-462, 1962.

7. Birrel, K. S. and Fieldes, M. Allophane in Volcanic Ash Soils. J. Soil Sci. 3:156-166, 1952.

8. Blake, G. R. "Bulk Density," Black, C. A., Ed., Methods of Soil Analysis. No. 9 Monograph Series, Amer. Soc. Agron. pp. 381-383, 1965.

9. Bradley, W. F. and Grim, R. E. "Mica Clay Minerals," Brown, G., Ed., The X-ray Identification and Crystal Structures of Clay Minerals. Mineral. Soc., London, pp. 208-239, 1961.

10. Brand, J. P. and DeFord, R. K. Geology of Eastern Half of Kent Quadrangle, Culberson, Reeves, and Jeff Davis Counties, Texas. Publ. by Bureau of Economic Geology, Univ. of Texas, Quad. Map No. 24, 1962.

11. Brewer, R. Fabric and Mineral Analysis of Soils. John Wiley and Sons, Inc., New York, 470 p., 1964.

12. Buondonno, C. and Violante, P. Il Terreno della Valle dell' Irno. Agrochimica. 11:65-78, 1966.

13. Carloni, L. and Lotti, G. Le Argille dei Terreni Provenienti dalle Trachiti Toscane. Agrochimica. 4:110-118, 1960.

14. DeFord, R. K. Tertiary Formations of the Rim Rock Country, Presidio County, Trans-Pecos, Texas. Texas J. Sci. 10:1-37, 1958a.

15. _____ Cretaceous Platform and Geosyncline of Culberson and Hudspeth Counties, Trans-Pecos, Texas. Trans-Pecos Guidebook, 1958 Field Trip. Publ. by Permian Basin Section, Society of Economic Paleontologists and Mineralogists, p. 28, 1958b.

16. Eifler, G. K., Jr. Geology of the Barrilla Mountains, Texas. Geol. Soc. Amer. Bull. 69:339-353, 1951.

17. Goldich, S. S. and Seward, C. Green Valley-Paradise Valley Trip. West Texas Geol. Soc., Guidebook Fall Field Trip. pp. 11-36, 1948.

18. Grim, R. E. Clay Mineralogy. McGraw-Hill Book Co., Inc., New York, 384 p., 1953.

19. Gruver, R. M. Precision Method of Thermal Analysis. J. Amer. Ceram. Soc. 31:323-328, 1948.

20. Hashimoto, I. and Jackson, M. L. "Rapid Dissolution of Allophane and Kaolinite-Halloysite after Dehydration," Ingerson, E., Ed., Proc. 7th Natl. Conf. on Clays and Clay Minerals. Pergamon Press, New York, pp. 102-113, 1960.

21. Hay-Roe, H. Geology of Wylie Mountains and Vicinity, Culberson and Jeff Davis Counties, Texas. Publ. by Bureau of Economic Geology, Univ. of Texas, Quad. Map No. 21, 1957.

22. Hess, P. C. Phase Equilibria of Some Minerals in the K_2O Na_2O Al_2O_3 SiO_2 H_2O System at 25 C and 1 Atmosphere. Amer. J. Sci. 264:289-309, 1966.

23. Huang, W. T. and Craft, J., Jr. Geomorphic and Structural Relationships of Tertiary Volcanic Rocks in Alpine and Vicinity, West Texas. Geol. Soc. Amer. Bull. 69:1589-1590, 1958.

24. Jackson, M. L. and Mackenzie, R. C. "Chemical Analysis in the Quantitative Mineralogical Examination of Clays," Rich, C. I. and Kunze, G. W., Eds., Soil Clay Mineralogy. The Univ. of North Carolina Press, Chapel Hill, pp. 315-316, 1964.

25. Jones, C. T. Cretaceous and Eocene Stratigraphy of Barrilla and Eastern Davis Mountains of Trans-Pecos, Texas. Amer. Ass. of Pet. Geol. Bull. 22:1423-1439, 1938.

26. Kilmer, V. J. The Estimation of Free Iron Oxides in Soils. Soil Sci. Soc. Amer. Proc. 24:420-421, 1960.

27. Kilmer, V. J. "Silicon," Black, C. A., Ed., Methods of Soil Analysis. No. 9 Monograph Series, Amer. Soc. Agron. pp. 961-962, 1965.

28. Kilmer, V. J. and Alexander, L. T. Methods of Making Mechanical Analyses of Soils. Soil Sci. 68:15-24, 1949.

29. Kinter, E. B. and Diamond, S. A New Method for Preparation and Treatment of Oriented - Aggregate Specimans of Soil Clays for X-ray Diffraction Analyses, Soil Sci. 81:111-120, 1956.

30. Mackenzie, R. C. and Mitchell, B. D. "Apparatus and Technique for Differential Thermal Analysis," MacKenzie, R. C. Ed., The Differential Thermal Investigation of Clays. Mineral. Soc., London, pp. 23-64, 1957.

31. Marel, H. W. van der. Volcanic Glass, Allanite and Zircon as Characteristic Minerals of the Toba Rhyolite at Sumatra's East Coast. J. Sedimentary Petrol. 18:24-29, 1948.

32. Marshall, C. E. The Physical Chemistry and Mineralogy of Soils. John Wiley and Sons, Inc., New York, pp. 80-90, 1964.

33. McAnulty, W. N. Geology of Cathedral Mountain Quadrangle, Brewster County, Texas. Geol. Soc. Amer. Bull. 66:531-578, 1955.

34. McLean, E. O. "Aluminon," Black, C. A.,Ed., Methods of Soil Analysis. No. 9 Monograph Series, Amer. Soc. Agron. pp. 988-990, 1965.

35. Prince, A. L. "Methods in Soil Analysis," Bear, F. E., Ed., Chemistry of the Soil. Reinhold Publ. Corp., New York, pp. 328-331, 1958.

36. Sellards, E. H., Adkins, W. S. and Plummer, F. B. The Geology of Texas. Univ. of Texas Pub. 3232: Publ. by Bureau of Economic Geology, Univ. of Texas, 1932.

37. Soil Survey Staff, Soil Classification, A Comprehensive System, 7th Approximation, U.S. Government Printing Office, Washington, 1960.

38. Stotzky, G. and DeMumbrum, L. E. Effect of Autoclaving on X-ray Characteristics of Clay Minerals. Soil Sci. Soc. Amer. Proc. 29:225-227, 1965.

39. Swindale, L. D. and Jackson, M. L. A Mineralogical Study of Soil Formation in Four Rhyolite-Derived Soils from New Zealand. New Zeal. J. Geol. Geophys. 3:141-183, 1960.

40. Texas Almanac 1965-1966, Publ. by the Dallas Morning News, Dallas, Texas, 735 p., 1966.

41. Theisen, A. A. and Harward, M. E. A Paste Method for Preparation of Slides for Clay Mineral Identification by X-Ray Diffraction. Soil Sci. Soc. Amer. Proc. 26:90-91, 1962.

42. United States Salinity Laboratory Staff, Diagnosis and Improvement of Saline and Alkali Soils, U.S.D.A. Handbook 60, Richards, L. A., Ed., U.S. Government Printing Office, Washington, 1954.

43. Vogel, F. A., Jr. Preliminary Report on the Rutile and Kaolin Deposits of the Medley District in Jeff Davis County, Texas. Mineral Resource Surv. Circ. No. 53. Publ. by Bureau of Economic Geology, Univ. of Texas, 1942.

44. Webber, L. R. and Shivas, J. A. The Identification of Clay Minerals in Some Ontario Soils: I. Parent Materials. Soil Sci. Soc. Amer. Proc. 17:96-99, 1953.